

# The Coalescence of Intrahost HIV Lineages Under Symmetric CTL Attack

Sivan Leviyang  
Georgetown University  
Department of Mathematics

February 17, 2022

## Abstract

Cytotoxic T lymphocytes (CTLs) are immune system cells that are thought to play an important role in controlling HIV infection. We develop a stochastic ODE model of HIV-CTL interaction that extends current deterministic ODE models. Based on this stochastic model, we consider the effect of CTL attack on intrahost HIV lineages assuming CTLs attack several epitopes with equal strength. In this setting, we introduce a limiting version of our stochastic ODE under which we show that the coalescence of HIV lineages can be described by a simple paintbox construction. Through numerical experiments, we show that our results under the limiting stochastic ODE accurately reflect HIV lineages under CTL attack when the HIV population size is on the low end of its hypothesized range. Current techniques of HIV lineage construction depend on the Kingman coalescent. Our results give an explicit connection between CTL attack and HIV lineages.

## 1 Introduction

Cytotoxic T lymphocytes (CTLs) are immune system cells that kill pathogen infected host cells. In the context of HIV infection, considerable experimental evidence suggests that CTLs play a central role in controlling infection and shaping HIV diversity, e.g. [3, 4, 11, 18, 33].

Roughly, when HIV enters a host cell, typically a  $CD4^+$  cell, certain mechanisms within the cell cut up HIV proteins into small pieces (usually 8 – 11 amino acids long) and present these peptides on the surface of the cell in the form a peptide-MHC complex (pMHC) [6]. CTLs can bind to pMHC complexes and then destroy the presenting cell, but critically each CTL possesses receptors that can bind to a limited pattern of peptides. An HIV peptide that is attacked by CTLs is referred to as an *epitope*.

When CTLs attack a given epitope, HIV infected cells possessing that epitope are killed off. However, due to its high mutation rate, many variants of HIV exist during any moment of infection. As a result, infected

cells possessing HIV variants that do not produce the attacked epitope may exist prior to CTL attack or arise during the attack. Such variants, which are at a selective advantage due to the CTL attack, will proliferate and come to dominate the HIV population. This hypothetical picture has been confirmed in many experimental HIV studies, e.g. [15]. Yet despite the putative role of CTLs in controlling HIV infection and the corresponding importance of HIV genetic diversity in evading CTL attack, the impact of CTL attack on intrahost HIV genetic diversity is not well understood.

Most current theoretical tools used in HIV research do not link CTL models to HIV genetic diversity. On one hand, HIV-CTL interaction has been modeled since the beginning of the HIV epidemic (see [25, 27] for a review). Various models are possible, but the standard model consists of a deterministic ODE composed of variables for the population size of HIV virions, infected and uninfected  $CD4^+$  cells, and CTLs targeting infected  $CD4^+$  cells. While the standard model and its many variations give a dynamic picture of HIV and CTL population sizes, they do not connect CTL attack to HIV population genetics.

On the other hand, tools from population genetics that do not explicitly model CTL attack have been applied to HIV. Rodrigo and coworkers used variants of the Kingman coalescent to explore the HIV life cycle and construct inference algorithms based on HIV genetic samples [31, 30, 8]. The popular programs BEAST and LAMARC, which are used to make statistical inferences based on HIV genetic data, assume a Kingman coalescent [7, 19].

In this work, we present results that connect an ODE model of HIV population dynamics under CTL attack to HIV population genetics. More specifically, we consider a stochastic ODE that models HIV escape from CTL attack at multiple epitopes sometime during the chronic phase of infection. Our stochastic ODE describes the dynamics of the HIV population in terms of discrete birth, death, and mutation events, allowing us to specify lineages once the dynamics are given. We show that under a certain small population limit our stochastic ODE connects to the deterministic ODE models described above.

To connect to HIV population genetics, we consider a collection of HIV infected cells sampled after HIV has escaped CTL attack. Given a realization of the stochastic ODE dynamics, the lineages of these infected cells can be traced back to the time at which CTL attack initiates, thereby forming a genealogy. For simplicity, we assume CTL attack of equal strength at each considered epitope, a situation we refer to as symmetric attack. In this setting, our main result characterizes the state of the genealogy at the time when CTL attack initiates. Further, we show that HIV escape mutations produce significant stochasticity in the HIV population dynamics.

We analyze our stochastic ODE using methods similar to those used by Iwasa, Michor, Komarova, and Nowak [13] and Durrett, Schmidt, and Schweinsberg [9] in their study of cancer pathways. Hermisson and Pennings [12, 26] also used similar techniques in an abstract setting applicable to HIV. In all these works and our own, the dynamics of mutations present at low levels in the overall population are well approximated by branching

processes. Rouzine and Coffin considered an HIV model that bears some similarity to our HIV-CTL model [32], but their analysis and goals differ from ours.

Our lineage construction is similar in spirit to that of several authors, but there are significant differences between our underlying model and that of previous authors. In [14, 10] the authors considered lineages from a population that has undergone a strong selective sweep, while in [2] the authors considered lineages from a population under selection-mutation equilibrium. Both these works considered a fixed size, Moran model with weak mutation rates. In our case, the stochastic ODE considered does not assume a fixed population size and we consider a strong mutation rate reflective of HIV biology.

In section 2 we describe our model. In section 3 we describe our theoretical results along with associated numerical results. In section 4 we discuss some implications of our results. Sections 5 and 6 provide proofs of the results presented in Section 3. In these two sections, we have endeavored to focus on the intuition behind the proofs. Our hope is that the mathematics presented in these sections contributes to intuition and biological motivation. We place arguments that are mathematically technical, and unnecessary for intuition, in the appendix.

## 2 A Model of HIV Dynamics Under CTL Attack

To specify our model, in section 2.1 we introduce terminology that will help characterize the CTL attack. In section 2.2, we introduce our stochastic ODE model and connect it to a deterministic ODE similar to those mentioned in the introduction. In section 2.3, we specify a specific parameter choice for our stochastic ODE that models symmetric CTL attack. Finally, in section 2.4, we discuss genealogies within the context of our HIV-CTL model.

### 2.1 Escape Graph

We model an HIV population exposed to attack at  $\mathbf{e}$  epitopes. To do this, we categorize the HIV infected cells by the presence, represented by a  $\mathbf{0}$ , or absence, represented by a  $\mathbf{1}$ , of a given epitope. Since there are  $\mathbf{e}$  epitopes, the different HIV infected cell variants can be associated with a binary number of length  $\mathbf{e}$ . For example if  $\mathbf{e} = 2$ , then the HIV infected cell variant, hereafter we simply say variant,  $\mathbf{10}$  represents an infected cell containing only the second epitope. Intuitively, we think of  $\mathbf{1}$ 's as representing mutations that alter a gene on the HIV genome that is responsible for producing the attacked epitope.

We let  $\mathcal{E}$  be the set of possible variants. In this work, we focus on two possible choices for  $\mathcal{E}$ . In the first, which we label as  $\mathcal{E}_{\text{full}}$ , we consider every possible combination of epitopes. For example, if  $\mathbf{e} = 3$  we define

$$\mathcal{E}_{\text{full}} = \{\mathbf{000}, \mathbf{001}, \mathbf{010}, \mathbf{011}, \mathbf{100}, \mathbf{101}, \mathbf{110}, \mathbf{111}\}. \quad (2.1)$$

In the second choice, which we label as  $\mathcal{E}_{\text{linear}}$ , we consider only variants that, from left to right, contain a sequence of all **1**'s followed by a sequence of all **0**'s. In the case  $\mathbf{e} = 3$  we define

$$\mathcal{E}_{\text{linear}} = \{\mathbf{000}, \mathbf{100}, \mathbf{110}, \mathbf{111}\} \quad (2.2)$$

Given  $\mathcal{E}$  we define a graph  $G$  which we call the *escape graph* of  $\mathcal{E}$ .  $G$  is formed from vertices labeled by elements of  $\mathcal{E}$  and arrows that connect a vertex with label  $v'$  to one with label  $v$  if a single epitope mutation can change  $v'$  to  $v$ . When  $\mathcal{E} = \mathcal{E}_{\text{full}}$  and  $\mathcal{E} = \mathcal{E}_{\text{linear}}$  we refer to the associated  $G$  as the *full* and *linear escape graph*, respectively. Figures 1 and 2 show the full and linear escape graph, respectively, in the case  $\mathbf{e} = 3$ .

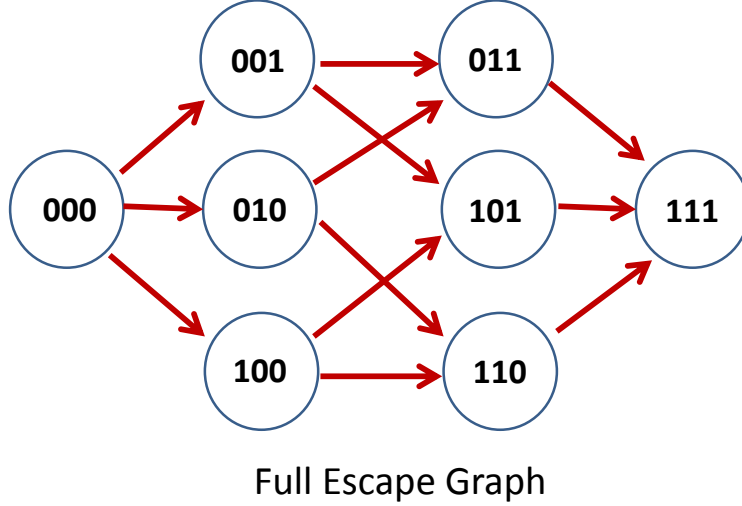


Figure 1: Full Escape Graph for  $\mathbf{e} = 3$ .

For any  $v \in \mathcal{E}$ ,  $\mathcal{P}(v)$  is the set of elements in  $\mathcal{E}$  that can be changed into  $v$  by transforming a single **0** into a **1**. Intuitively, we think of  $\mathcal{P}(v)$  as the variants that can be transformed into  $v$  by a single mutation and the  $\mathcal{P}$  stands for parents. To be clear, if  $v = \mathbf{110}$  then we have  $\mathcal{P}(v) = \{\mathbf{010}, \mathbf{100}\}$  and  $\mathcal{P}(v) = \{\mathbf{100}\}$  for the full and linear escape graphs respectively.

We say that the HIV population has escaped CTL attack when all infected cells are of type **111...1**. In other words, mutations that remove each of the attacked epitopes have fixed in the HIV population.

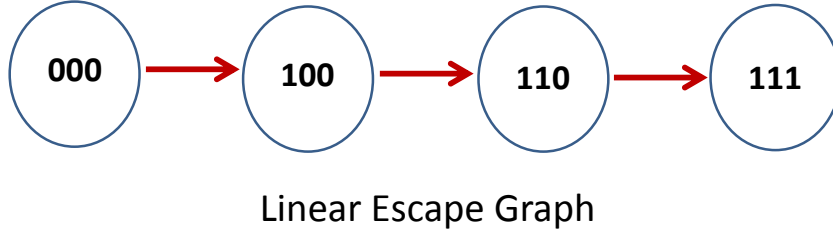


Figure 2: Linear Escape Graph for  $\mathbf{e} = 3$ .

## 2.2 ODE

Let  $h$  represent the number of uninfected  $\text{CD4}^+$  cells that are targets for HIV infection. For each  $v \in \mathcal{E}$  let  $e_v$  be the number of  $\text{CD4}^+$  cells infected by  $v$  variants. We assume birth and death rates for  $h$  and the  $e_v$  as specified in Table 1.  $\lambda$  and  $g$  represent the birth and death rates respectively of a  $\text{CD4}^+$  cell in the absence of HIV infection.  $b_v h$  and  $k_v$  are the birth and death rate of a  $v$  variant, infected  $\text{CD4}^+$  cell. An infected  $\text{CD4}^+$  birth event corresponds to an uninfected  $\text{CD4}^+$  death event, so uninfected  $\text{CD4}^+$  cells have an additional death term beyond  $g$ .

We let  $\mu$  be the rate per infection event at which mutations occur that remove any one of the  $\mathbf{e}$  epitopes. Correspondingly, new  $v$  variants arise from mutations in  $v' \in \mathcal{P}(v)$  with a rate given in the 'mutation event' rate column in Table 1. Notice that a 'mutation event' in Table 1 refers to the creation of a  $v$  variant from a mutation in some variant contained in  $\mathcal{P}(v)$ , not the mutation of a  $v$  variant itself.

Define  $P(f(t))$  to be a Poisson process with jump rate  $f(t)$  at time  $t$ .

cell type (# of cells)	birth rate	death rate	mutation event
uninfected ( $h$ )	$\lambda$	$g + \sum_{v \in \mathcal{E}} b_v e_v$	-
$v$ infected ( $e_v$ )	$b_v h$	$k_v$	$\mu \sum_{v' \in \mathcal{P}(v)} b_{v'} e_{v'} h$

Table 1: Birth, Death, and Mutation Rates

Then, given the rates in Table 1 we have the following stochastic ODE,

$$\begin{aligned} dh &= dP(\lambda) - dP(gh) - \sum_{v' \in \mathcal{E}} dP(b_{v'} e_{v'} h) \\ de_v &= dP(b_v e_v h) - dP(k_v e_v) + \sum_{v' \in \mathcal{P}(v)} dP(\mu b_{v'} e_{v'} h). \end{aligned} \quad (2.3)$$

where the second equation directly above applies for all  $v \in \mathcal{E}$ . Each  $P$  in (2.3) represents an independent Poisson process run at the specified rate, to avoid cumbersome notation we do not use a distinct notation for each of these processes. In (2.3) and throughout this work, we ignore back mutations, a mutation from a variant to a less fit variant. Ignoring such mutations does not affect our results.

To make our system variables ( $h$  and the  $e_v$ )  $O(1)$ , we rescale  $h$  and each  $e_v$  by  $\mathbb{H}$  and  $\mathbb{E}$  respectively. Intuitively,  $\mathbb{H}$  and  $\mathbb{E}$  correspond to the order at which uninfected but infectable  $\text{CD4}^+$  cells and infected, activated  $\text{CD4}^+$  cells capable of producing virions exist during HIV infection, respectively. We set  $\mathbb{H} = \lambda/g$ , the steady state of uninfected cells in the absence of HIV infection. This scaling is supported by empirical results suggesting that, at least prior to AIDS onset, the number of uninfected  $\text{CD4}^+$  cells during and prior to HIV infection are on the same order [5]. Without justification for a moment, we choose  $\mathbb{E} = g/\bar{b}$  where  $\bar{b}$  is on the order of the  $b_v$ . If we rewrite  $h$  and  $e_v$  as  $h/\mathbb{H}$  and  $e_v/\mathbb{E}$  respectively in (2.3), we arrive at the rescaled system,

$$\begin{aligned} dh &= \frac{g}{\lambda} \left( dP(\lambda) - dP(\lambda h) - \sum_{v' \in \mathcal{E}} dP(\lambda \frac{b_{v'}}{\bar{b}} e_{v'} h) \right) \\ de_v &= \frac{\bar{b}}{g} \left( dP(\lambda \frac{b_v}{\bar{b}} e_v h) - dP\left(\left(\frac{k_v g}{\bar{b}}\right) e_v\right) + \sum_{v' \in \mathcal{P}(v)} dP(\mu \lambda \frac{b_{v'}}{\bar{b}} e_{v'} h) \right). \end{aligned} \quad (2.4)$$

We would like to recover a deterministic ODE from (2.4), in this way showing that our present model is an extension of current deterministic models. In [20], Kurtz showed that one can recover deterministic population ODEs by taking large population limits of stochastic population ODEs. In our context, we can consider  $\mathbb{H} \rightarrow \infty$  and  $\mathbb{E} \rightarrow \infty$ . Such limits are reasonable for HIV due to its enormous population size, but it is not immediately clear what the relationship should be between  $\mathbb{H}$  and  $\mathbb{E}$  as both go to infinity.

To address this issue in a simple context, consider (2.4) without CTL attack. In this setting we need not distinguish between different variants, reducing our system to the variables  $h$  and  $e$ , and we may also ignore

mutation. Taking  $\mathbb{H}$  and  $\mathbb{E}$  large, we can largely ignore the stochasticity of (2.3) and arrive at the following deterministic ODE,

$$\begin{aligned}\frac{dh}{dt} &= g(1 - h - eh) \\ \frac{de}{dt} &= \frac{b}{g}e(\lambda h - \frac{kg}{b}),\end{aligned}\tag{2.5}$$

which has the equilibrium,

$$h = (kg)/(b\lambda)\tag{2.6}$$

Consider the variables in the expression for  $h$  directly above.  $k$ , the death rate of infected  $\text{CD4}^+$  cells has been measured at approximately 2 days [28]. If we take 2 days as our time scale, we then expect  $k \approx 1$ . Uninfected  $\text{CD4}^+$  cells last on the order 2 weeks, giving  $g = .1$  as a reasonable choice. Estimates for  $b$  and  $\lambda$  have significant variation in the literature. However, we can understand the role of  $\lambda$  and  $b$  in (2.4) by noting the following relation,

$$\lambda b = g^2 \left( \frac{\mathbb{H}}{\mathbb{E}} \right),\tag{2.7}$$

which follows from our formulas for  $\mathbb{H}$  and  $\mathbb{E}$ . The above relation and (2.6) demonstrate that (2.4) only converges to a deterministic system in the large population limit of  $\mathbb{H}, \mathbb{E} \rightarrow \infty$  if the ratio  $\mathbb{H}/\mathbb{E}$  converges to a fixed constant.

To force (2.4) to have a deterministic limit, we introduce a parameter  $\gamma = \lambda b/g$  or in terms of  $\mathbb{H}, \mathbb{E}$ ,  $\gamma = g(\mathbb{H}/\mathbb{E})$  (the factor  $g$  is not essential, but gives the system directly below a simpler form). From a biological point of view,  $\gamma$  is an inverse measure of the fraction of infectable cells that are actually infected. Empirical results for the ratio of infected to infectable cells are difficult as most infected  $\text{CD4}^+$  are in the lymph nodes and many such  $\text{CD4}^+$  are infected but inactive [22]. However, estimates in the range of .01 to .1 have been given by several authors and seem reasonable [22]. With  $g = .1$ , the corresponding range for  $\gamma$  is 1 to 10. Using this scaling of  $\gamma$ , our definition of  $\mathbb{E}$  is justified biologically.

Rewriting (2.4) using  $\gamma$  and setting  $\tilde{b}_v = b_v/\bar{b}$  gives

$$\begin{aligned}dh &= \frac{1}{\mathbb{E}} \left( \frac{g}{\gamma} \right) \left( dP(\gamma\mathbb{E}) - dP(\gamma\mathbb{E}h) - \sum_{v' \in \mathcal{E}} dP(\tilde{b}_{v'}\gamma\mathbb{E}e_{v'}h) \right) \\ de_v &= \frac{1}{\mathbb{E}} \left( dP(\gamma\tilde{b}_v\mathbb{E}e_vh) - dP(k_v\mathbb{E}e_v) + \sum_{v' \in \mathcal{P}(v)} dP(\mu\tilde{b}_{v'}\gamma\mathbb{E}e_{v'}h) \right).\end{aligned}\tag{2.8}$$

and we consider the limit of this system as  $\mathbb{E} \rightarrow \infty$ .

*While (2.8) approaches a deterministic limit as  $\mathbb{E} \rightarrow \infty$  when mutation is ignored, the system will continue to be stochastic if  $\mu$  is sufficiently large with respect to  $\mathbb{E}$ .* Indeed, as we show in section 3, the scaling of  $\mu$  that produces stochasticity is precisely a scaling in which HIV lives. Roughly, stochasticity of (2.8) exists even as  $\mathbb{E} \rightarrow \infty$  because the dynamics of variants that are of scaled population size  $O(\frac{1}{\mathbb{E}})$ , i.e.  $e_v = O(\frac{1}{\mathbb{E}})$ , will be stochastic even as  $\mathbb{E} \rightarrow \infty$ .

However, if we ignore mutation then as  $E \rightarrow \infty$ , (2.8) becomes

$$\begin{aligned}\frac{dh}{dt} &= g(1 - h - \sum_{v' \in \mathcal{E}} \tilde{b}_{v'} e_{v'} h) \\ \frac{de_v}{dt} &= \gamma(\tilde{b}_v h e_v - k_v e_v),\end{aligned}\tag{2.9}$$

which has the form of a predator-prey system. (2.9) is a simplified version of the standard deterministic ODE used today for HIV modeling, the full version includes the virion population. But generally, the reduction to (2.9) demonstrates how (2.8) is based on current HIV models.

### 2.3 Symmetric CTL Attack and Initial Conditions

We consider (2.8) restricted to the case of symmetric attack. To make the notion of symmetric attack precise, we partition the collection of variants,  $\mathcal{E}$ , into subsets  $\mathcal{E}_i$  such that

$$\mathcal{E}_i = \{v \in \mathcal{E} : v \text{ has } i \text{ 1's in its binary expression}\} \tag{2.10}$$

For example, if  $\mathbf{e} = 4$ , then  $\mathcal{E}_1 = \{\mathbf{1000}, \mathbf{0100}, \mathbf{0010}, \mathbf{0001}\}$  and  $\mathcal{E}_1 = \{\mathbf{1000}\}$  for the full and linear escape graph, respectively.  $\mathcal{E}_i$  is the collection of variants that are mutated at  $i$  epitopes. We refer to the  $\mathcal{E}_i$  generally as *variant classes* and  $\mathcal{E}_i$  specifically as the  *$i$ th variant class*.

To model symmetric attack, we assume that a variant  $v \in \mathcal{E}_i$  will be exposed to CTL attack at  $\mathbf{e} - i$  epitopes, and we assume that the death rate due to CTLs at each single epitope has rate  $\Delta k$ . We scale time so that infected cells die, in the absence of CTL attack, at rate 1. As mentioned, the lifetime of an infected cell has been shown to be approximately 2 days which is in turn our unit of time. All this is made precise by taking the death rate  $k_v$  of  $v \in \mathcal{E}_i$  to be given by

$$k_v = 1 + (\mathbf{e} - i)\Delta k. \tag{2.11}$$

Finally, as an added simplification, we take  $b_v$  to be constant. In (2.8) this amounts to taking  $\tilde{b}_v = 1$ .

Before presenting our final system, we note that mutations do not play a role in the equation for  $h$  and so stochastic effects will have little impact on  $h$  dynamics. For simplicity, and with error that goes to 0 as  $\mathbb{E} \rightarrow \infty$ , we replace the  $h$  equation by its deterministic counterpart. Putting all these remarks together, we arrive at the following system.

$$\begin{aligned}\frac{dh}{dt} &= g \left( 1 - h - \sum_{v' \in \mathcal{E}} e_{v'} h \right) \\ de_v &= \frac{1}{\mathbb{E}} \left( dP(\gamma \mathbb{E} e_v h) - dP(k_v \mathbb{E} e_v) + \sum_{v' \in \mathcal{P}(v)} dP(\mu \gamma \mathbb{E} e_{v'} h) \right).\end{aligned}\tag{2.12}$$

From this point on, we take (2.12) as describing the dynamics of the HIV population.



To set initial conditions, we assume that variant  $v_0 = \mathbf{000}\dots\mathbf{0}$  is the dominant variant prior to CTL attack. Indeed, CTLs proliferate in response to epitopes existing in the population, so taking  $v_0$  to be the dominant variant is biologically reasonable. Ignoring other variants for a moment, we set  $h, e_{v_0}$  at time  $t = 0$  according to the equilibrium of (2.5):

$$\begin{aligned} h(0) &= \frac{1}{\gamma}, \\ e_{v_0}(0) &= \frac{1 - h(0)}{h(0)}. \end{aligned} \tag{2.13}$$

Prior to CTL attack, we assume that other variants are at a slight fitness disadvantage to  $v_0$  and arise due to mutations on  $v_0$  variants. Assuming, as we have just done, that there are  $O(\mathbb{E})$   $v_0$  variants, there will be  $O(\mu\mathbb{E})$  variants from each of the  $\mathcal{E}_1$  classes. From this, we can conclude that the number of variants in the  $\mathcal{E}_2$  class will be of order  $O(\mu^2\mathbb{E})$ . As we mention below,  $\mu^2\mathbb{E} \approx 0$  and so we assume that no  $\mathcal{E}_i$  variants exist at  $t = 0$  for  $i > 1$ . For simplicity we assume  $e_v(0) = \mu\mathbb{E}$  for all  $v \in \mathcal{E}_1$ .

These initial conditions are not essential to our results, other choices are possible. Which initial conditions are appropriate will depend on the period of HIV infection one has in mind. We have made a specific choice for the sake of clarity.

## 2.4 Genealogies

When all variants are of type  $\underbrace{\mathbf{11}\dots\mathbf{1}}_e$ , the HIV population has escaped CTL attack. We let  $T_{\text{sample}}$  be a time after such an escape has been completed and consider  $n$  infected cells sampled at  $T_{\text{sample}}$ . Since (2.12) defines discrete birth and death events, we can construct lineages corresponding to the ancestral lines of these  $n$  sampled cells.

We label the lineages  $\ell_1, \ell_2, \dots, \ell_n$  and we let  $\Pi(t)$  represent the partition structure of the lineages at time  $t$ . To explain this, consider Figure 3 which represents a possible lineage structure for the case  $n = 8$ . The values of  $\Pi(t)$  at  $t = T_{\text{sample}}, T_B, T_C$  are given by,

$$\begin{aligned} \Pi(T_{\text{sample}}) &= \{\{\ell_1\}, \{\ell_2\}, \dots, \{\ell_8\}\} \\ \Pi(T_B) &= \{\{\ell_1, \ell_2\}, \{\ell_3, \ell_4\}, \{\ell_5, \ell_6\}, \{\ell_7, \ell_8\}\} \\ \Pi(T_C) &= \{\{\ell_1, \ell_2, \ell_3, \ell_4, \ell_5, \ell_6\}, \{\ell_7, \ell_8\}\} \end{aligned}$$

At time  $T_{\text{sample}}$  all lineages are separate,  $\Pi(T_{\text{sample}})$  consequently partitions each lineage into its own set. By time  $T_B$ , the pairs of lineages 1 and 2, 3 and 4, 5 and 6, and 7 and 8 have coalesced.  $\Pi(T_B)$  partitions these pairs to reflect this structure. Finally by time  $T_C$ , lineages 1 through 6 have coalesced as has the pair 7 and 8.  $\Pi(T_C)$  partitions the lineages accordingly.

$\Pi(t)$  is a random partition function that encodes the genealogy formed by the  $n$  lineages. Its stochasticity follows from the stochasticity of (2.12) as well as the stochasticity of lineages given a single realization of (2.12)

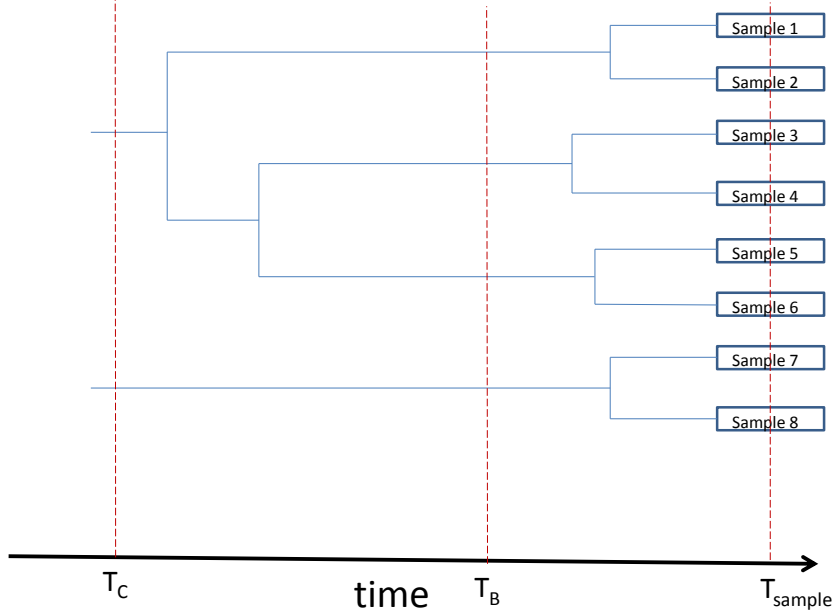


Figure 3: Example Lineages.  $n = 8$

### 3 Results

Our results characterize the lineage structure at  $t = 0$  of  $n$  infected cells sampled at  $t = T_{\text{sample}}$ , a time after HIV has escaped CTL attack. More precisely, Theorems 3.1 and 3.2, provide a random partition to which  $\Pi(0)$  converges in the limit  $\mathbb{E} \rightarrow \infty, \mu \rightarrow 0$  with the limit taken so that  $\mu^3 \mathbb{E}^2 \rightarrow 0$  and  $\mu \mathbb{E} \rightarrow \infty$ . We refer to this limit as the *small population limit*, **SPL**. Throughout this work, whenever we take an unspecified limit, we mean the SPL.

In experimental and theoretical HIV studies,  $\mathbb{E}$  has been estimated in the range  $10^6 - 10^8$ . In [34], the number of activated  $\text{CD4}^+$  cells with integrated provirus was found to average  $3 \times 10^7$ . Various studies have estimated that somewhere between 1 in 1000 to 1 in 80000  $\text{CD4}^+$  cells are productively infected during HIV infection, see p. 91 in [22] and references therein. Using a base of  $10^{11}$  infectable lymphocytes [22], this gives a range of approximately  $10^6 - 10^8$  for  $\mathbb{E}$ . Presumably,  $\mathbb{E}$  varies depending on the individual and stage of infection. Mutation rates for HIV per base pair per infection event have been estimated at approximately  $10^{-5}$  [5]. Through numerical experiments, we show that Theorems 3.1 and 3.2, exact in the SPL, are a good approximation for the lineage structure formed under (2.12) in the parameter regime  $\mu = 10^{-5}$ ,  $\mathbb{E} = 10^6$ . In contrast, we show that the parameter regime  $\mu = 10^{-5}$ ,  $\mathbb{E} = 10^8$  is not well approximated

by the SPL. The regime  $\mu = 10^{-5}$ ,  $\mathbb{E} = 10^7$  is a middle ground in which the SPL is a reasonable approximation, but significant error does exist. Therefore, we think of the SPL as being a limiting version of (2.12) when HIV has a relatively small infected cell population size.

Theorems 3.1 and 3.2 do not specify the structure of  $\Pi(t)$  at times other than  $t = 0$ . However, the arguments we use to justify these theorems do provide some results in this direction which we mention in the Discussion section. Similarly, while our results focus on lineage structure, we make some observations regarding the stochastic dynamics of (2.12) in the Discussion section. As we mentioned in section 2.2, the  $\mathbb{E} \rightarrow \infty$  limit does not eliminate the stochasticity of (2.12) in certain parameter regimes for  $\mu$  and the SPL is one such a regime.

In section 3.1, we present our SPL results, while in section 3.2 we discuss the numerical results that connect the SPL to the parameter regimes of HIV.

### 3.1 Small Population Limit Results

The dynamics of (2.12) are composed of successive sweeps in which each variant class displaces the previous variant class as the dominant portion of the infected cell population. For example, Figure 4 shows a realization of (2.12) for a full escape graph with  $e = 5$ ,  $\Delta k = .1$ ,  $\gamma = 3$ ,  $g = .1$ ,  $\mu = 10^{-5}$ ,  $\mathbb{E} = 10^7$ . The figure was generated by solving (2.12) numerically.

Since initially there are no variants outside of the 0th and 1st variant classes, the variants from the  $i$ th variant class with  $i > 1$  come from  $\mathcal{E}_{i-1} \rightarrow \mathcal{E}_i$  mutations, i.e. a mutation  $v' \rightarrow v$  with  $v' \in \mathcal{E}_{i-1}$  and  $v \in \mathcal{E}_i$ . The SPL scaling forces such mutations to occur during a time interval when  $\mathcal{E}_{i-2}$  variants dominate the population and  $\mathcal{E}_{i-1}, \mathcal{E}_i$  variants are at low frequencies. During this time interval, all variants in  $\mathcal{E}_j$  with  $j < i - 2$  have been driven out of the population, or nearly so, while all variants in  $\mathcal{E}_j$  for  $j > i$  have yet to arise. We refer to this time interval as the  $\mathcal{E}_{i-1}$  *spawning phase* because the rise in  $\mathcal{E}_i$  variants is being driven by  $\mathcal{E}_{i-1} \rightarrow \mathcal{E}_i$  mutations. At later times, once the  $\mathcal{E}_i$  population has reached higher frequencies,  $\mathcal{E}_{i-1} \rightarrow \mathcal{E}_i$  mutations have little impact on  $\mathcal{E}_i$  variant population dynamics and the  $\mathcal{E}_{i-1}$  spawning phase ends. The condition  $\mu^3 \mathbb{E}^2 \rightarrow 0$  in the SPL insures that a variant that is being spawned cannot simultaneously spawn another variant.

During the  $\mathcal{E}_{i-1}$  spawning phase, variants in  $\mathcal{E}_{i-1}$  are increasing in population size at approximately rate  $\Delta k$  while variants in  $\mathcal{E}_i$  are increasing at approximately rate  $2\Delta k$ . To see why, recall that the  $\mathcal{E}_{i-2}$  variants dominate the infected cell population during the  $\mathcal{E}_{i-1}$  spawning phase. Since  $\mathcal{E}_{i-1}$  and  $\mathcal{E}_i$  variants are attacked by CTLs at 1 less and 2 less epitopes than  $\mathcal{E}_{i-2}$  variants, their relative fitness is given by  $\Delta k$  and  $2\Delta k$  respectively. These dynamics are a generalized version of the well studied Luria-Delbrück (LD) model (see [36] for an excellent review of LD models and results). The LD model assumes a wild type population growing at rate, say,  $a$  that produces mutant types that also grow at rate  $a$ . This contrasts to the growth rates  $\Delta k, 2\Delta k$  for  $\mathcal{E}_{i-1}$  and  $\mathcal{E}_i$  variants respectively in the  $i - 1$ th spawning phase. For this reason, we refer to spawning phase dynamics as obeying a generalized LD model. The dynamics of the LD

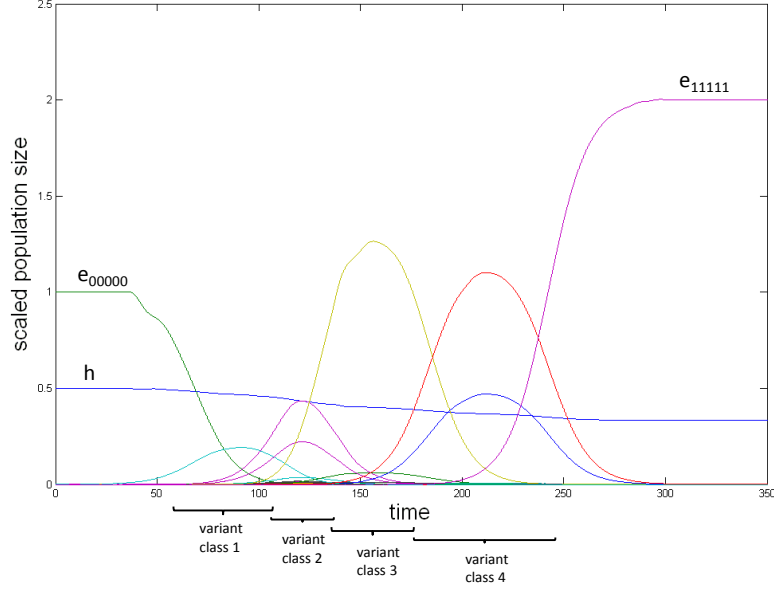


Figure 4: Dynamics of (2.12) for a full escape graph with  $\mathbf{e} = 5$ ,  $\Delta k = .1$ ,  $\gamma = 3$ ,  $\mu = 10^{-5}$ ,  $\mathbb{E} = 10^7$ .

model have been studied for many years and the LD distribution, which gives the number of mutant types at a given time, is well understood.

We analyze (2.12) by decomposing the time considered,  $[0, T_{\text{sample}}]$ , into a series of time intervals  $[T_i, T_{i+1}]$  for  $i = 0, 1, \dots, \mathbf{e} - 2$  along with intervals  $[0, T_0]$ ,  $[T_{\mathbf{e}-1}, T_{\mathbf{e}}]$  and  $[T_{\mathbf{e}}, T_{\text{sample}}]$ . The interval  $[T_i, T_{i+1}]$  is the  $\mathcal{E}_{i+1}$  spawning phase. Intervals  $[0, T_0]$ ,  $[T_{\mathbf{e}-1}, T_{\mathbf{e}}]$ ,  $[T_{\mathbf{e}}, T_{\text{sample}}]$  are boundary cases that do not correspond to a spawning phase. In this way, we reduce (2.12) to a sequence of spawning phases.

For each vertex  $v$ , we define the *pop value* of  $v$  as the number of  $v$  variants at the beginning of the  $v$  spawning phase. More precisely, if  $v \in \mathcal{E}_{i+1}$  then the pop value of  $v$  is  $e_v(T_i)$  because  $T_i$  is the beginning of  $v$ 's spawning phase. For the linear escape graph, we can express the distribution of the  $v$ th pop value through a simple formula that is independent of other pop values, see (5.6). In the case of a full escape graph, the distribution of the  $v$ th pop value is given by an iterative formula that depends on other pop values, see (6.2).

Pop values help us get a handle on the stochasticity of (2.12). As  $\mathbb{E}$  becomes large, the stochasticity of (2.12) becomes restricted to variants of small population size. In our terminology, the stochasticity of (2.12) becomes restricted to spawning phases and their corresponding general-

ized LD dynamics. For an interval  $[T_i, T_{i+1}]$ , pop values describe variant population sizes at  $T_i$  and  $T_{i+1}$ , thereby giving us a handle on the LD dynamics that occur between these two times.

We use extensions of previous LD results to derive our pop value formulas. However, these formulas connect to dynamics and we are interested in forming lineages. Correspondingly, we need to understand not only the dynamics of the LD model but also how to construct lineages on a generalized LD model. The random partition  $\Xi_{A,i}$ , which we discuss more thoroughly below, characterizes the coalescent events on lineages as they move backwards in time through generalized LD dynamics corresponding to a single spawning phase. To form lineages, we consider a sequence of spawning phases. For a linear escape graph, this is done through simple concatenation of  $\Xi_{A,i}$ . But for the full escape graph, things are more complicated as variants within a variant class affect each others dynamics and hence each others lineages.

### 3.1.1 linear escape graph

As mentioned, constructing lineages for linear escape graphs is just a matter of concatenating the coalescent events associated with each spawning phase. We characterize such coalescent events through the random partition  $\Xi_{A,i}$  which we now define.

For  $i = 0, 1, \dots, e - 2$  we define a r.v.  $\Gamma^{(i)}$  by,

$$\Gamma^{(i)} = \exp[2 * W_1] W_2 B\left(\frac{2\Delta k}{k_i}\right). \quad (3.14)$$

where  $W_1, W_2$  are independent exponential r.v.'s with mean 1 and  $B(p)$  is an independent Bernoulli r.v. with success probability  $p$ .

We define  $\Xi_{A,i}$  through a paintbox construction as follows (see [17, 29] for a review of paintbox constructions).

**Definition 1.** Let  $A > 0$  and  $i \in \{0, 1, \dots, e - 2\}$  be given. Then we define a partition  $\Xi_{A,i}(S)$  on any set  $S$  as follows. Let  $K$  be a sample from a Poisson r.v. with mean  $A$ . For  $j = 1, 2, \dots, K$  we sample  $\Gamma_j$  from the r.v.  $\Gamma^{(i)}$ .

Thinking of the  $j$  as colors, we 'paint' each  $s \in S$  a random color according to the probability

$$P(\text{paint with color } j) = \frac{\Gamma_j}{\sum_{j'=1}^K \Gamma_{j'}} \quad (3.15)$$

The partition  $\Xi_{A,i}(S)$  is formed by grouping together elements sharing the same color.

The  $K$  samples of  $\Gamma^{(i)}$  correspond to  $K, \mathcal{E}_{i+1} \rightarrow \mathcal{E}_{i+2}$  mutations on the  $\mathcal{E}_{i+1}$  spawning phase,  $[T_i, T_{i+1}]$ . Each  $\Gamma^{(i)}$  sample is proportional to the number of descendants at  $T_{i+1}$  produced by a single such mutation. Essentially, the  $\Gamma^{(i)}$  samples provide a decomposition for the pop value of  $v \in \mathcal{E}_{i+2}$ . More precisely,

$$e_v(T_{i+1}) = C \sum_{j=1}^K \Gamma_j, \quad (3.16)$$

where  $C$  is a constant independent of  $j$ . The decomposition (3.16) allows us to construct lineages, while simply sampling the pop value would not. Roughly, the number of infected cells at  $T_{i+1}$  that descend from the  $j$ th  $\mathcal{E}_{i+1} \rightarrow \mathcal{E}_{i+2}$  mutation is proportional, with constant  $C$  in (3.16), to  $\Gamma_j$ . This means that a sampled cell will descend from mutation  $j$  with probability given by (3.15). Sampled cells that descend from the same mutation on  $[T_i, T_{i+1}]$  must coalesce during that period. In this way  $\Xi_{A,i}$  characterizes coalescent events on  $[T_i, T_{i+1}]$ .

The parameter  $A$  is a tuning parameter. As Theorem 3.1 shows, raising  $A$  improves accuracy by considering more mutations, but at a computational cost of increasing the number of  $\Gamma^{(i)}$  samples that must be taken.

For the linear escape graph,  $\Pi(0)$  is simply a concatenation of the  $\Xi_{A,i}$ .

**Theorem 3.1.** *Consider (2.12) assuming a linear escape graph. Then letting  $\Delta$  be any partition of the  $n$  lineages,*

$$\lim P(\Pi(0) = \Delta) = P\left(\prod_{i=0}^{e-2} \Xi_{A,i}\right)(\Pi(T_{\text{sample}})) = \Delta) + O\left(\frac{1}{A}\right) \quad (3.17)$$

where  $\Xi_{A,i}$  is given by definition 1.

Recall that  $\Pi(T_{\text{sample}})$  simply partitions each lineage separately since no coalescent events have occurred. By  $(\prod_{i=0}^{e-2} \Xi_{A,i})(\Pi(T_{\text{sample}}))$  we mean the concatenation of the  $\Xi_{A,i}$  applied to  $\Pi(T_{\text{sample}})$ . For example if  $e = 3$  then,

$$\left(\prod_{i=0}^1 \Xi_{A,i}\right)(\Pi(T_{\text{sample}})) = \Xi_{A,0}(\Xi_{A,1}(\Pi(T_{\text{sample}}))). \quad (3.18)$$

### 3.1.2 full escape graph

As mentioned, the  $i+1$ th spawning phase involves  $\mathcal{E}_{i+1} \rightarrow \mathcal{E}_{i+2}$  mutations. For the linear escape graph, there is only one variant in each variant class, meaning that there is only one type of  $\mathcal{E}_{i+1} \rightarrow \mathcal{E}_{i+2}$  mutation. However, for the full escape graph we must consider  $v' \rightarrow v$  mutations for every  $v \in \mathcal{E}_{i+2}$  and  $v' \in \mathcal{P}(v)$ . The time period  $[T_i, T_{i+1}]$  will be composed of many concurrent spawning phases, one for each such  $v' \rightarrow v$ .

To explain the generalization of Theorem 3.1 to the full escape graph, recall that for the linear escape graph  $\Xi_{A,i}$  is formed by taking  $K$  samples of  $\Gamma^{(i)}$  and  $K$  is always sampled from a Poisson r.v. with mean  $A$ . In the full escape graph case, for each  $v \in \mathcal{E}_{i+2}, v' \in \mathcal{P}(v)$  we take  $K_{v' \rightarrow v}$  samples of  $\Gamma^{(i)}$ , where  $K_{v' \rightarrow v}$  is sampled from a Poisson r.v. with mean that depends on the pop value of  $v'$  relative to the other vertices in the  $\mathcal{E}_{i+1}$  class.

To explain why  $K_{v' \rightarrow v}$  should depend on pop values, consider  $v', v'' \in \mathcal{P}(v)$ . Suppose  $e_{v'}(T_i) \gg e_{v''}(T_i)$ . In other words,  $v'$  has a much higher pop value than  $v''$ . A higher pop value will mean that on  $[T_i, T_{i+1}]$ , more  $v' \rightarrow v$  mutations occur than  $v'' \rightarrow v$  mutations and correspondingly we should have  $K_{v' \rightarrow v} > K_{v'' \rightarrow v}$ . This effect did not arise in the linear escape graph because each variant class contains a single variant.

Since  $K_{v' \rightarrow v}$  depends on pop values, intuitively we must first sample pop values and then construct the  $K_{v' \rightarrow v}$ . However, as in (3.16),

to form lineages we do not sample pop values. Rather we decompose each pop value according to the number of descendants produced by each  $v' \rightarrow v$  mutation. The decomposition depends on  $K_{v' \rightarrow v}$ . Putting these comments together, we must build  $K_{v' \rightarrow v}$  and pop value decompositions simultaneously. This is done in Definition 2. The variable  $D_v$  is proportional to the pop value of  $v$  and is formed through a decomposition analogous to (3.16).

**Definition 2.** For each  $v \in \mathcal{E}_1$  we define  $D_v = 1$ . Then we recursively define  $D_v$ ,  $K_{v' \rightarrow v}$  and  $\Gamma^{(i)}$  samples as follows. Suppose the  $D_v$  values are known for  $v \in \mathcal{E}_{i-1}$ . Set

$$D_{\max, i-1} = \max_{v \in \mathcal{E}_{i-1}} D_v \quad (3.19)$$

For each  $v \in \mathcal{E}_i$  and  $v' \in \mathcal{P}(v)$  we let  $K_{v' \rightarrow v}$  be a sample from a Poisson r.v. with mean  $A(D_{v'}/D_{\max, i-1})$ . For each  $j = 1, 2, \dots, K_{v' \rightarrow v}$ , we sample  $\Gamma_{v' \rightarrow v, j}$  from  $\Gamma^{(i)}$ . Then,

$$D_v = \sum_{v' \in \mathcal{P}(v)} \sum_{j=1}^{K_{v' \rightarrow v}} \Gamma_{v' \rightarrow v, j} \quad (3.20)$$

The above definition allows us to define  $K_{v' \rightarrow v}$  and  $\Gamma$  samples for every mutation pair  $v' \rightarrow v$ . The pop value of  $v \in \mathcal{E}_{i+1}$  is given by,

$$e_v(T_i) = C_i D_v = C_i \sum_{v' \in \mathcal{P}(v)} \sum_{j=1}^{K_{v' \rightarrow v}} \Gamma_{v' \rightarrow v, j}, \quad (3.21)$$

where  $C_i$  depends only on  $i$ . (3.21) is analogous to (3.16).

For the full escape graph, the state of our lineages is not simply a partition of  $\{\ell_1, \ell_2, \dots, \ell_n\}$ . Rather, we must specify a vertex to which each lineage is associated at a given time  $t$ . Intuitively, the vertex associated with, say,  $\ell_j$  at time  $t$  is the variant type of the infected cell at time  $t$  from which the  $j$ th sampled cell descends. To put this in the context of a partition function,  $\Pi(t)$  partitions the lineages into disjoint sets and associates with each such set a vertex in  $\mathcal{E}$ . The  $\Xi_{A, i}$  defined below are random partitions on sets for which every element is associated with a vertex in  $\mathcal{E}_{i+2}$ .

**Definition 3.** We define a partition  $\Xi_{A, i}(S)$  on a set  $S$  for which each element  $s \in S$  is associated with a vertex  $v_s \in \mathcal{E}_{i+2}$ . For every  $s, v_s$  pair and  $v' \in \mathcal{P}(v_s)$  let  $K_{v' \rightarrow v_s}$ ,  $D_{v_s}$  and associated  $\Gamma_{v' \rightarrow v_s, j}$  be as defined in Definition 2. Assign a unique color to every triple  $(v', v_s, j)$ . Then we paint each element  $s \in S$  the color associated with  $(v', v_s, j)$  and assign it element  $v'$  with the following probabilities,

$$P(\text{paint with color } (v', v_s, j) \text{ and assign vertex } v') = \frac{\Gamma_{v' \rightarrow v_s, j}}{D_{v_s}} \quad (3.22)$$

The partition  $\Xi_{A, i}(S)$  is formed by grouping together elements sharing the same color.

With the adjusted definition of  $\Xi_{A, i}$ , the statement of Theorem 3.1 now holds for the full escape graph.

regime	$\mu$	$\mathbb{E}$	$\mu^3 \mathbb{E}^2$	$\mu \mathbb{E}$
SPL	-	-	0	$\infty$
AR	$10^{-10}$	$10^{13}$	.0001	1000
SPR	$10^{-5}$	$10^6$	.001	10
MPR	$10^{-5}$	$10^7$	.1	100
LPR	$10^{-5}$	$10^8$	10	1000

Table 2: Parameter Regimes

**Theorem 3.2.** *Consider (2.12) assuming a full escape graph. Then letting  $\Delta$  be any partition of the  $n$  samples,*

$$\lim_{SPL} P(\Pi(0) = \Delta) = P\left(\prod_{j=0}^{e-2} \Xi_{A,i}\right) (\Pi(T_{\text{sample}})) = \Delta) + O\left(\frac{1}{A}\right) \quad (3.23)$$

where  $\Xi_{A,i}$  is given by definition 3

For the full escape graph,  $\Pi(T_{\text{sample}})$  partitions each lineage separately and assigns to each lineage the vertex  $\mathbf{11} \dots \mathbf{1}$  since we sample after HIV has escape CTL attack.  $\Delta$  should assign to each lineage a variant of class  $\mathcal{E}_0$  or  $\mathcal{E}_1$  since these are the only variants extant at  $t = 0$ . However, for simplicity Theorem 3.2 refers to the partition structure of the lineages at  $t = 0$ . (If we wanted to include the variant associated with each lineage at  $t = 0$ , we would need a  $\Xi_{A,-1}$ . Our methods allow for this, but for the sake of simplicity and because our initial conditions are slightly ad-hoc, we do not consider such an extension.)

## 3.2 Numerical Results

In this section we consider five parameter regimes: the approximating regime (AR), the small population regime (SPR), the medium population regime (MPR), and the large population regime (LPR). Table 2 specifies the  $\mu$  and  $\mathbb{E}$  value associated with each regime. The table also includes the corresponding values for  $\mu^3 \mathbb{E}^2$  and  $\mu \mathbb{E}$ . The AR has  $\mu^3 \mathbb{E}^2 \ll 1$  while  $\mu \mathbb{E} \gg 1$ , suggesting a good approximation by the SPL. Notice that the SPR has a scaling near the SPL, but that the LPR has a  $\mu^3 \mathbb{E}^2$  value of 10 which, as we shall show, is too large for the SPL to apply.

To understand the accuracy of the SPL, we first consider the probability that two sampled lineages coalesce. More precisely, setting  $n = 2$  we consider the probability that  $\ell_1$  and  $\ell_2$  coalesce by  $t = 0$  or equivalently  $P(\Pi(0) = \{\{\ell_1, \ell_2\}\})$ . This probability is often computed in population genetics applications and is one way to characterize  $\Pi(0)$  [35]. Figure 5 shows this coalescent probability for a linear escape graph with  $\gamma = 3$  and  $\Delta k = .1$ . The x-axis gives the number of epitopes in the linear escape graph, our parameter  $\mathbf{e}$ . We skip  $\mathbf{e} = 1$  because due to our initial conditions such an attack has a coalescent probability near zero. For each value of  $\mathbf{e}$  considered, we computed five quantities given by the five bars. The left most bar represents the coalescent probability given in the SPL, as specified through Theorem 3.1. To compute the coalescent probability



in this case, we set  $A = 100$ , higher values of  $A$  don't change the result, and constructed  $\Xi_{A,i}$  for  $i = 0, 1, \dots, e - 2$ . This amounts to sampling the r.v.'s  $\Gamma^{(i)}$ . We generated 1000 realizations of the sequence of  $\Xi_{A,i}$ . For each realization, we then applied the paintbox construction implied by the underlying  $\Gamma^{(i)}$  samples to determine if the two lineages coalesced. We did this 1000 times for each realization of the  $\Xi_{A,i}$ . In this way we computed one million 1's, for coalescence, and 0's, for non-coalescence. Averaging this list gave us the coalescent probability.

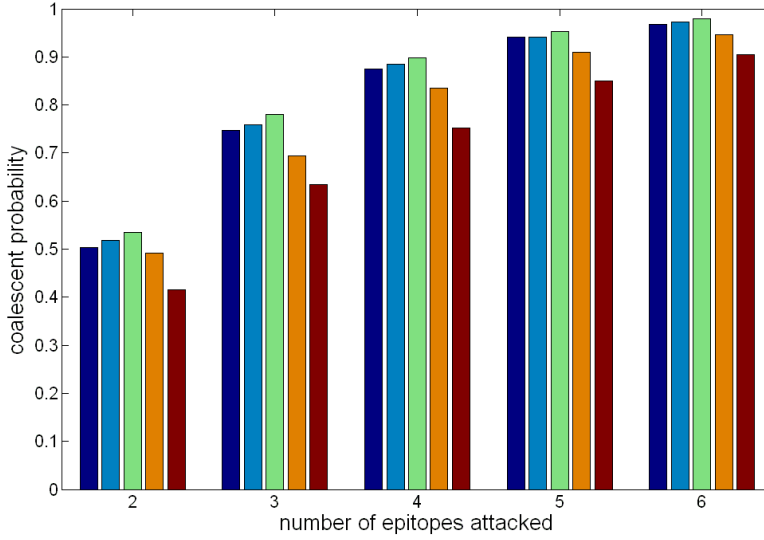


Figure 5: The probability of coalescence of two lineages for a linear escape graph with  $\gamma = 3$ ,  $g = .1$ ,  $\Delta k = .1$ . The bars, from left to right, give the coalescent probability under the SPL, AR, SPR, MPR, and LPR (see Table 2 for the definition of these parameter regimes).

The next four bars represent, from left to right, the coalescent probability for the AR, SPR, MPR and LPR, respectively. These values are computed by solving (2.12) numerically and forming lineages on top of the stochastic dynamics. We compute 1000 realizations of (2.12) dynamics, and for each such realization we consider the coalescence of 2 lineages 1000 times. We then average over all 1000 lineage pairs and all 1000 realizations. Solving (2.12) and building lineages on top of the dynamics is not numerically trivial due to the large population size. Following methods described in [21], we solve (2.12) exactly and track parent-child relationships in each variant until the variant population size exceeds 10000. At

that point we switch to the deterministic ODE analogue of (2.12).

As Figure 5 demonstrates, the SPL is a good approximation in the AR and SPR, but not the LPR. The MPR represents a middle ground. Figure 6 is the same as Figure 5, except that in Figure 6, we consider a full escape graph.

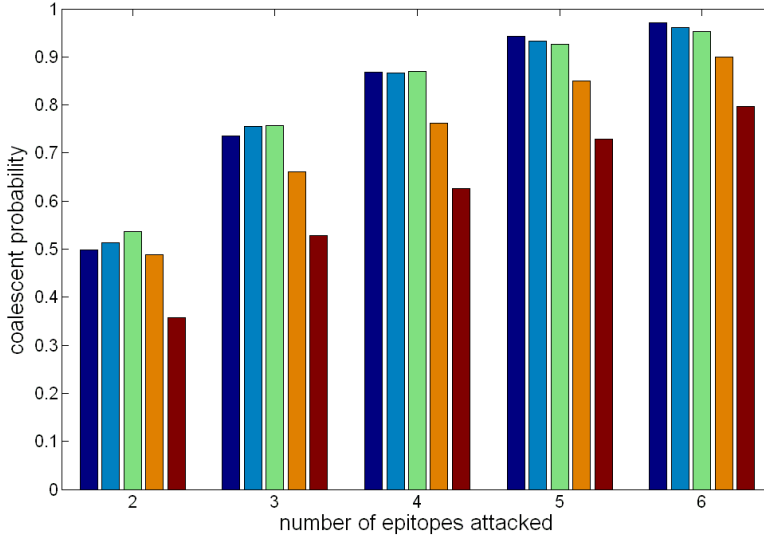


Figure 6: The probability of coalescence of two lineages for a full escape graph with  $\gamma = 3$ ,  $g = .1$ , and  $\Delta k = .1$ . The bars, from left to right, give the coalescent probability under the SPL, AR, SPR, MPR, and LPR (see Table 2 for the definition of these parameter regimes).

Another value that can be used to characterize the HIV genealogy shaped by CTL attack is the number of still uncoalesced lineages at  $t = 0$ . More precisely, we consider the number of elements in  $\Pi(0)$ . Recall that each element of  $\Pi(0)$  is a collection of lineages that have coalesced. Figure 7 shows the distribution of this number for a full escape graph with  $\mathbf{e} = 3$ ,  $\gamma = 10$ ,  $\Delta k = .3$  and  $n = 100$ . The same pattern of accuracy is seen as with Figures 5 and 6.

Theorems 3.1 and 3.2 provide a theoretical framework for understanding genealogies on (2.12). However, they also provide a computational approach for sampling such genealogies that is much faster than solving (2.12) directly. Table 3 gives the CPU time in seconds required to generate the coalescent probability results shown in Figures 5 and 6 for the cases  $\mathbf{e} = 2, 6$ . We show CPU times needed to produce the probability through

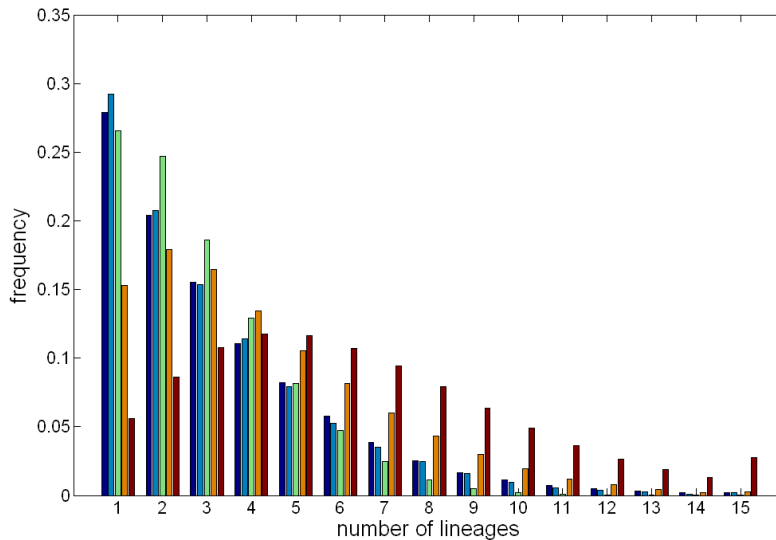


Figure 7: The number of uncoalesced lineages at  $t = 0$  assuming a sample of 100 infected cells after HIV escape. Results correspond to a full escape graph with  $\mathbf{e} = 3$ ,  $\gamma = 10$  and  $\Delta k = .3$ . The bars, from left to right give values under the SPL, AR, SPR, MPR, and LPR (see Table 2 for the definition of these parameter regimes).

our SPL results and by solving (2.12) in the SPR, the times required for the APR, MPR, and LPR are similar to the SPR. As can be seen, the SPL approach is more than 300 times faster in the case of a full escape graph and  $\mathbf{e} = 6$ . For the linear escape graph and the  $\mathbf{e} = 2$  full escape graph, the SPL approach is on the order of 100 times faster.

## 4 Discussion

Application of the results we have presented depends on approximating the SPL scaling by satisfying  $\mu\mathbb{E} \gg 1$  and  $\mu^3\mathbb{E}^2 \ll 1$ . HIV almost certainly always satisfies  $\mu\mathbb{E} \gg 1$ , so this condition is not restrictive. On the other hand,  $\mu^3\mathbb{E}^2 \ll 1$  is satisfied if the HIV population size is of relatively small magnitude, namely on the order of  $10^6$ . Importantly, the HIV population size we must consider is the number of active  $\text{CD4}^+$  cells infected with functioning HIV genome. Inactivated  $\text{CD4}^+$  cells or those infected by non-functional HIV do not enter into our model because they do not produce offspring infected cells.

graph	$\epsilon$	SPL time	SPR time	SPR/SPL
LINEAR	2	29	4700	162
	6	135	11300	84
FULL	2	32	5300	165
	6	159	54000	340

Table 3: CPU Time in seconds needed to generate coalescent probabilities. CPU is an Intel-Celeron single node processor.

Our results have implications for both dynamics and genealogies. For dynamics, our arguments show that the stochasticity of (2.12) in the SPL is completely contained within the pop values described in the results section and defined precisely in (5.6) and (6.2). Intuitively, once a variant population reaches large size, averaging effects take over and deterministic dynamics apply. In our nomenclature, a variant population is small and hence experiences stochastic dynamics only when it is being spawned by another variant population. These spawning dynamics are encoded in the pop values which are stochastic. Taking all this together, if we are interested in dynamics and not lineages, then (2.12) can be reduced to a deterministic ODE accompanied by stochastic pop values.

The stochasticity of the pop values has significant impact on the dynamics of (2.12). Figure 8 gives a solution for the deterministic analogue of (2.12) in which stochastic events are replaced by their average. Another way to describe such a system is as (2.12) when all pop values are equal. Either way, since our equations are symmetric, the dynamics must be symmetric and this is indeed the case in Figure 8. All variants within the same variant class have identical dynamics.

In contrast, Figure 9 provides the dynamics for a single realization of (2.12). We can see that stochasticity plays an essential role in (2.12) because Figure 9 gives very different dynamics than Figure 8. But further, our work explains the stochasticity seen in Figure 9. In a given variant class, some variants have higher pop values than others. Such variants dominate the others in their class. For example in Figure 9, the variant **011** dominates **110**, **101** when these variants compose most of the population. This dominance results from stochasticity corresponding to a high pop value. Biologically, the stochasticity of pop values come from the stochasticity of mutation times.

Turning now to genealogies, we have described the coalescence of lineages caused by the whole period of HIV escape. However, as mentioned, we can decompose HIV escape into time intervals  $[T_i, T_{i+1}]$ . Each such period corresponds to  $\Xi_{A,i}$  and so we know the state of the lineages at each  $T_i$  given the state at  $T_{i+1}$ . Between the  $T_i$ , however, our results do not describe the lineages. Figures 10 and 11 show genealogies formed for a 5 epitope and 2 epitope attack, respectively, in the case of a linear escape graph under the SPR. Here we have shown all coalescent events that happen during  $[T_i, T_{i+1}]$  to occur at  $T_i$ . Both genealogy figures were produced using Figtree. (Figtree is available as part of the BEAST software package [7].)

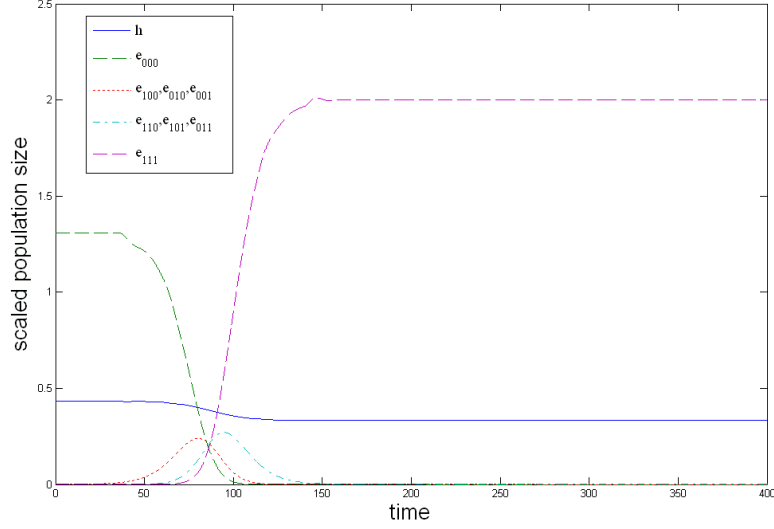


Figure 8: (2.12) run deterministically for a full escape graph with  $\mathbf{e} = 3$ ,  $\Delta k = .1$ ,  $\gamma = 3$ ,  $\mu = 10^{-5}$ ,  $\mathbb{E} = 10^6$ . As a consequence of symmetry, all variants in the same epitope class evolve identically.

The restriction of our current results to symmetric attack and the small end of the HIV population size range is a significant limitation. Further work should allow for these restriction to be lifted, but our current results provide some general observations.

For a full escape graph, the assumptions of symmetric attack makes the paths through the graph identical in terms of the underlying parameters. Removal of the symmetric attack assumption would lead to a dominant path. For example, if there is an epitope that is attacked more strongly than the other epitopes, then it will be the first epitope at which HIV escapes CTL attack. Of course, there will be some HIV variants that initially possess a mutation at a different epitope, but these will be few in number. The order of the epitopes at which HIV escapes from the CTL attack will be specified in the case of asymmetric CTL attack. As a result, HIV escape on a full escape graph in the asymmetric attack case should proceed essentially on one path of the graph and be similar to the linear escape graph dynamics and genealogies we have discussed.

Our numeric results allow us to compare the form of genealogies for large and small HIV populations. Figure 12 compares coalescent probabilities for linear and full escape graphs. This is the same data presented

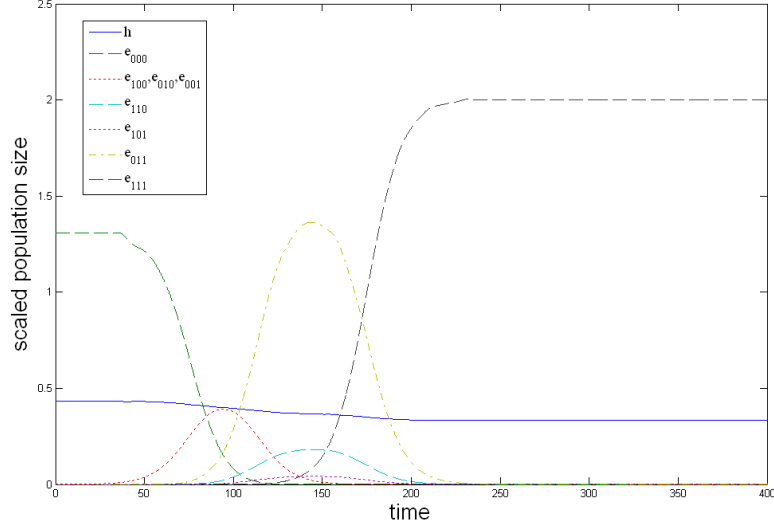


Figure 9: (2.12) run for a full escape graph with  $\mathbf{e} = 3$ ,  $\Delta k = .1$ ,  $\gamma = 3$ ,  $\mu = 10^{-5}$ ,  $\mathbb{E} = 10^6$ . Unlike the deterministic case shown in Figure 8, the symmetry of the model is broken by stochastic effects.

in Figures 5 and 6. In Figure 12 the four bars give, from left to right, the coalescent probability for a linear escape graph under SPR, a full escape graph under SPR, a linear escape graph under LPR, and a full escape graph under LPR. As can be seen, the coalescent probabilities under the SPR are similar for the linear and full escape graphs. Some numerical experiments suggest that this is because pop value stochasticity causes a single path through the full escape graph to dominate, similarly to our earlier comments on asymmetric attack. We don't know why this is not the case for the LPR. It may be that pop values take on a different form in this regime to which our SPL analysis does not apply.

## 5 Linear Escape Graph

In this section we consider (2.12) for the linear escape graph under the SPL. Our main aim is to explain and demonstrate Theorem 3.1. For notational simplicity, we set  $v_i = \underbrace{11 \dots 1}_{i} 00 \dots 0$ . In this subsection we

write  $e_i$  for  $e_{v_i}$  in (2.12). For each variant class  $\mathcal{E}_i$  we define  $T_i$  for  $i = 1, 2, \dots, \mathbf{e}$  as the time at which variant  $v_i$  reaches scaled population size

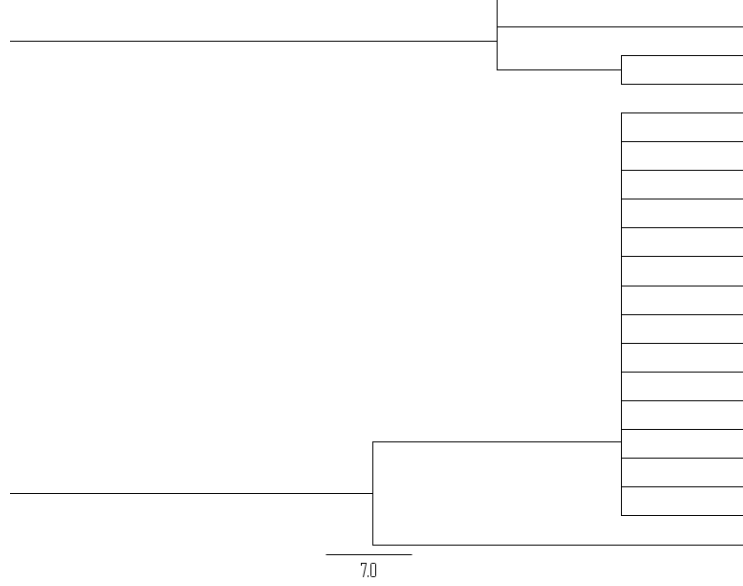


Figure 10: Sampled genealogy for a linear escape graph with 5 epitopes attacked under the SPR, that is  $\mu = 10^{-5}$ ,  $\mathbb{E} = 10^6$ .  $\gamma = 3$ ,  $g = .1$ , and  $\Delta k = .1$  as in Figure 5.  $n = 20$ . The time scale at the bottom is in units of 2 days.

$\delta$ ,

$$T_i = \inf\{t : e_{v_i} \geq \delta\}, \quad (5.1)$$

where

$$\delta = \left( \frac{1}{|\log(\mu^2 \mathbb{E})|} \right)^2 \quad (5.2)$$

The value of  $\delta$  can fall within a range of values, the formula above is a specific choice within this range. Intuitively,  $\delta$  represents a microscopic-macroscopic cutoff. Different variants 'interact' in (2.12) through the  $h$  equation. When a variant has population less than  $\delta$ , its impact on  $h$  dynamics and in turn on the dynamics of other variants is small and can be ignored in the SPL. From this perspective, the smaller  $\delta$  the better. On the other hand, a  $\delta$  that is too small will make the interval  $[T_i, T_{i+1}]$  too short in the sense that the  $v_{i+1} \rightarrow v_{i+2}$  mutations that drive the  $i + 1$ th spawning period will not have finished by  $T_{i+1}$ . From this perspective, the larger  $\delta$  the better. Our choice for  $\delta$  is a middle ground between these two extremes.

In the SPL,  $\delta \rightarrow 0$ . Variants with scaled population size less than  $\delta$  collapse as a percentage of the population in the SPL. This is why we think of  $\delta$  as a microscopic-macroscopic cutoff. However, if a variant has



Figure 11: Sampled genealogy for a linear escape graph with 2 epitopes attacked under the SPR, that is  $\mu = 10^{-5}$ ,  $\mathbb{E} = 10^6$ .  $\gamma = 3$ ,  $g = .1$ , and  $\Delta k = .1$  as in Figure 5.  $n = 20$ . The time scale at the bottom is in units of 2 days.

scaled population size  $\delta$  then the number of such variants, unscaled, is  $\delta\mathbb{E}$  which goes to  $\infty$  in the SPL. So while 'microscopic' variants are few as a percentage of the population, they may have large population sizes in an absolute sense.

We also set

$$T_0 = \inf\{t : e_1(t) = \mu^2 \mathbb{E} \delta^2\}. \quad (5.3)$$

$T_0$  is a special case because we set  $e_1(0) = \mu\mathbb{E}$ .

Using the  $T_i$  we decompose  $[0, T_{\text{sample}}]$  into intervals  $[T_{i-1}, T_i]$  along with initial and final intervals  $[0, T_0]$  and  $[T_{\mathbf{e}}, T_{\text{sample}}]$  respectively. That this composition is valid with probability 1 in the SPL, i.e.

$$P(T_0 < T_1 < \dots < T_{\mathbf{e}} < T_{\text{sample}}) \rightarrow 1, \quad (5.4)$$

will be a consequence of our analysis below.

We consider the interval  $[T_i, T_{i+1}]$  for  $i = 0, 1, \dots, \mathbf{e} - 2$ . The intervals  $[0, T_0]$ ,  $[T_{\mathbf{e}-1}, T_{\mathbf{e}}]$ ,  $[T_{\mathbf{e}}, T_{\text{sample}}]$  are handled separately. We show below that during  $[T_i, T_{i+1}]$ , only the variants  $v_{i-1}, v_i, v_{i+1}$  and  $v_{i+2}$  play a significant role in the dynamics. Table 4 shows the scaled population sizes of different variants at  $T_i$  and  $T_{i+1}$ . The arguments that justify Table 4 are given below, for now we focus on intuition.



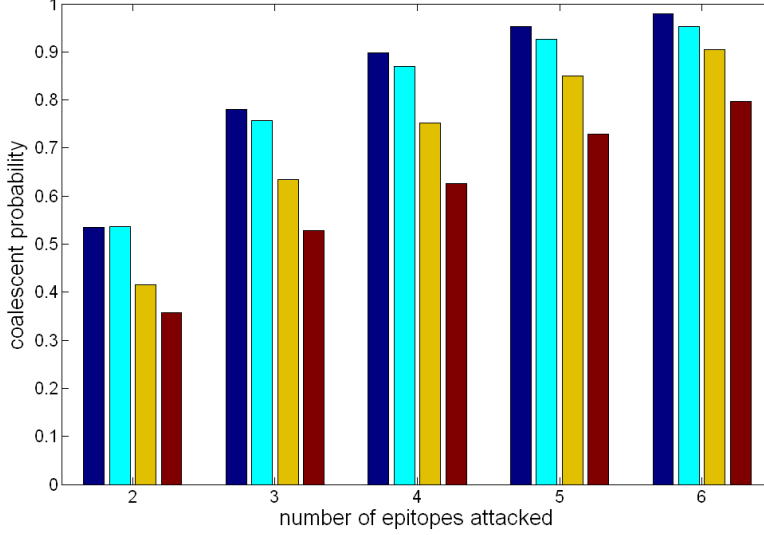


Figure 12: Comparison of the probability of coalescence of two lineages for a full escape graph and a linear escape graph with  $\gamma = 3$ ,  $g = .1$ , and  $\Delta k = .1$ . The bars, from left to right, give the coalescent probability under a linear escape graph and SPR, full escape graph and SPR, linear escape graph and LPR, and full escape graph and LPR (see Table 2 for the definition of these parameter regimes).

To explain Table 4, we first consider the  $v_{i-1}$  and  $v_i$  variants. If only one variant type exists in whole population, say  $v$ , then (2.12) is composed solely of the equations for  $h$  and  $e_v$  and in equilibrium we have  $e_v \approx (1 - h)/h$ . Examining Table 4, we see that at  $T_i$ ,  $v_{i-1}$  is roughly at this equilibrium, meaning that it is the dominant variant in the HIV population. On the other hand,  $v_i$  variants at time  $T_i$  are few since  $\delta \ll (1 - h)/h$ . However, by time  $T_{i+1}$ , the situation has flipped with  $v_i$  dominating the population and  $v_{i-1}$  pushed to low levels. Intuitively, the  $v_i$  variants are more fit and push out the  $v_{i-1}$  variants during  $[T_i, T_{i+1}]$ .

Now consider the  $v_{i+1}, v_{i+2}$  variants. Recalling that  $\mathbb{E}e_{i+1}(T_i)$  gives the number, unscaled, of  $v_{i+1}$  variants. We first note that

$$\mathbb{E}e_{i+1}(T_i) = O(\mu^2 \mathbb{E}^2 \delta^2) \ll \frac{1}{\mu}. \quad (5.5)$$

The  $\ll$  directly above is justified in the SPL since  $\mu^3 \mathbb{E}^2 \rightarrow 0$ . Since the probability of mutation is  $\mu$ , the inequality above shows that at  $T_i$  the

variant	$e.(T_i)$	$e.(T_{i+1})$
$v_{i-1}$	$(1 - h(T_i))/h(T_i) + O(\delta)$	$O(\delta)$
$v_i$	$\delta$	$(1 - h(T_{i+1}))/h(T_{i+1}) + O(\delta)$
$v_{i+1}$	$O(\mu^2 E \delta^2)$	$\delta$
$v_{i+2}$	0	$O(\mu^2 E \delta^2)$
$v_j$ for $j > i + 2$	0	0
$v_j$ for $j < i - 1$	$o(\delta)$	$o(\delta)$

Table 4: Dynamics of (2.12) during  $[T_i, T_{i+1}]$  for a linear escape graph.

rate of  $v_{i+1} \rightarrow v_{i+2}$  mutations goes to 0 in the SPL. However, notice that  $\mathbb{E}e_{i+1}(T_i) \approx O(\mu^2 \mathbb{E}^2) \rightarrow \infty$ , meaning that  $e_{i+1}$  dynamics are deterministic at time  $T_i$ .

Turning to  $v_{i+2}$  we see that at  $T_i$  no such variants exist. However, by time  $T_{i+1}$ , there are enough such variants to make their dynamics deterministic. Connecting to our comments in the Results section,  $[T_i, T_{i+1}]$  is the  $i + 1$ th spawning phase or, slightly more explicitly, the  $v_{i+1} \rightarrow v_{i+2}$  spawning phase.

Finally we note that Table 4 shows that all other variant types are of negligible population size.  $v_j$  with  $j > i + 2$  have yet to arise and  $v_j$  with  $j < i - 1$  have been previously driven to low levels by fitter variants.

Table 4 provides the outlines of an iteration, as we proceed through different values of  $i$ , that allows us to analyze the stochastic dynamics of (2.12). The key to deriving the table is an estimate of  $e_{i+2}(T_{i+1})$ , the pop value of  $v_{i+2}$ . In subsection 5.1 we show

$$\frac{e_{i+2}(T_{i+1})}{\mu \mathbb{E}^2 \delta^2} \rightarrow P_{i+2}, \quad (5.6)$$

where

$$P_{i+2} = \left( \frac{\Delta k}{k_i} \right)^2 \mathcal{S}\left(\frac{1}{2}, 1, \pi^2 \left( \frac{\Delta k}{k_i} \right)\right), \quad (5.7)$$

and where  $\mathcal{S}(\alpha, \beta, c)$  is the stable distribution with index  $\alpha$ , skewness parameter  $\beta$ , and scale factor  $c$  [24].

In subsection 5.1, we provide the arguments that justify Table 4 and (5.6). Then in section 5.2, we use the results of section 5.1, which center on the dynamics of (2.12), to demonstrate our lineage result, Theorem 3.1.

## 5.1 Dynamics

The goal of this section is to prove Proposition 1 which is a precise version of Table 4 and (5.6).

**Proposition 1.** *Consider (2.12) on a linear escape graph. Assume that at  $T_i$  for  $i = 1, \dots, e - 2$*

1.  $P(e_j(T_i) = 0) \rightarrow 1$  for  $j \geq i + 2$ .
2.  $\frac{e_{i+1}(T_i)}{\mu \mathbb{E}^2 \delta^2} \rightarrow P_{i+1}$

3.  $e_i(T_i) = \delta$
4.  $e_{i-1}(T_i) = \frac{1-h(T_i)}{h(T_i)} + O(\delta)$ .
5.  $e_j(T_i) = o(\delta)$  for  $j < i - 1$ .

Then at time  $T_{i+1}$  we have the following conclusions

1.  $P(e_j(T_{i+1}) = 0) \rightarrow 1$  for  $j \geq i + 3$ .
2. (5.6) holds
3.  $e_{i+1}(T_{i+1}) = \delta$
4.  $e_i(T_{i+1}) = \frac{1-h(T_{i+1})}{h(T_{i+1})} + O(\delta)$ .
5.  $e_j(T_{i+1}) = o(\delta)$  for  $j < i$ .

Conclusion 3 of Proposition 1 holds by the definition of  $T_{i+1}$ . Conclusions 4 and 5 could be phrased in terms of the SPL, for instance  $e_j(T_i)/\delta \rightarrow 0$ , but the  $o()$  notation is, to our taste, clearer.

We can apply Proposition 1 recursively to characterize the dynamics at each time  $T_i$  for  $i = 1, \dots, \mathbf{e} - 2$ . The case  $i = 0$ , which we must consider to start the recursion, is handled through the same arguments that give Proposition 1, except that our assumptions are slightly different. Namely, at  $T_0$  we have  $e_1(T_0) = \mu^2 \mathbb{E} \delta^2$  by definition of  $T_0$ , which parallels assumption 2 of Proposition 1 and  $e_0(T_0) = (1-h)/h + o(\delta)$  which parallels assumptions 3. Assumption 1 of Proposition 1 holds for the  $i = 0$  case, while assumptions 4 and 5 are not applicable.

To explain Proposition 1, we split  $[T_i, T_{i+1}]$  into two time intervals:  $[T_i, T_i^h]$  and  $[T_i^h, T_{i+1}]$ . In Lemma 5.1, we show that during  $[T_i, T_i^h]$  the  $v_i$  variant displaces the  $v_{i-1}$  variant as the dominant variant, as alluded to in Table 4 and the accompanying discussion. This transition happens quickly, so that  $T_i^h - T_i$  is small. As a result, the  $v_{i+1}$  population does not grow in size much and no  $v_{i+1} \rightarrow v_{i+2}$  mutations occur. Through the arguments of Lemma 5.2, we show that  $v_{i+1}, v_{i+2}$  dynamics on  $[T_i^h, T_{i+1}]$  obey the generalized LD dynamics discussed in the Results section.

**Lemma 5.1.** *Adopt the same assumptions stated in Proposition 1. Set  $T_i^h = T_i + (3/\Delta k + \frac{2}{\rho})|\log(\delta)|$  where  $\rho$  is given in (A.1.8). Then,*

1. for  $t \in [T_i, T_i^h]$ ,  $\mu \mathbb{E} e_{i+1}(t) \rightarrow 0$ ,
2.  $P(e_{i+2}(T_i^h) = 0) \rightarrow 1$ ,
3.  $e_i(T_i^h) = \frac{1-h(T_i^h)}{h(T_i^h)} + O(\delta)$
4.  $e_{i-1}(T_i^h) < \delta$ .

Conclusions 1 and 2 of Lemma 5.1 guarantee that no  $v_{i+1} \rightarrow v_{i+2}$  mutations occur during  $[T_i, T_i^h]$  and follow from the small population size of  $v_{i+1}$  variants at  $T_i$ . Indeed, by assumption we have  $e_{i+1}(T_i) = O(\mu^2 \mathbb{E} \delta^2)$ . The number of  $v_{i+1}$  variants grow exponentially on  $[T_i, T_i^h]$ . However,  $T_i^h - T_i = O(|\log(\delta)|)$  and so despite their exponential growth the number of  $v_{i+1}$  variants remains small. More precisely, referring to (2.12), we note that  $h$  is bounded above by 1 and so we can bound the exponential growth rate of  $e_{i+1}$  by  $\gamma$ ,

$$\frac{de_{i+1}}{dt} \leq \gamma e_{i+1}. \quad (5.8)$$

Integrating the above equation and using the assumption on  $e_{i+1}(T_i)$  gives,

$$e_{i+1}(t) \leq O(\mu^2 \mathbb{E} \delta^{2+\gamma}) \rightarrow 0, \quad (5.9)$$

where we have used the observation

$$\mu^2 E \ll (\mu^2 E) \mu E = \mu^3 \mathbb{E}^2 \rightarrow 0 \quad (5.10)$$

to justify convergence to 0 in the SPL. This gives conclusion 1.

Conclusion 2 follows almost directly from conclusion 1. We recall from (2.12) that  $v_{i+1} \rightarrow v_{i+2}$  mutations arise at rate  $\mu \mathbb{E} \gamma h e_{i+1}$ . The number of such mutations in the interval  $[T_i, T_i^h]$  is then a Poisson process with mean,

$$O(\mu \mathbb{E}) \int_{T_i}^{T_i^h} ds h(s) e_{i+1}(s) \quad (5.11)$$

Plugging in our bound from (5.9) shows the mean number of mutations to be bounded by  $O(\mu^3 E^2)$ , here we've ignored  $\delta$  factors. Taking the SPL gives conclusion 2.

To explain conclusions 3 and 4 of Lemma 5.1 we notice that only variants  $v_i$  and  $v_{i-1}$  are of order greater than  $\delta$  throughout  $[T_i, T_i^h]$ . Ignoring the other variants then, our ODE (2.12) reduces to three equations involving  $e_i, e_{i-1}, h$ . Since variant  $v_i$  has one less epitope exposed to CTL attack than  $v_{i-1}$ , it will eventually push the  $v_{i-1}$  to extinction. Initially,  $e_i(T_i) = \delta$ . Since the CTL kill rate of  $v_{i-1}$  variants is  $\Delta k$  greater than those of  $v_i$  variants, initially the  $v_i$  variants grow exponentially with rate  $\Delta k + O(\delta)$ . It then takes  $O(\frac{1}{\Delta k} |\log(\delta)|)$  time for the  $v_i$  population to rise to  $O(1)$  levels, push out the  $v_{i-1}$  population, and near equilibrium with respect to  $h$ . This explains the order of  $T_i^h$ . The exact form of  $T_i^h$  is explained in section A.1 of the appendix as are the technical details demonstrating conclusions 3 and 4.

Now we consider  $[T_i^h, T_{i+1}]$  through the following lemma.

**Lemma 5.2.** *Assume the conclusions of Lemma 5.1. Then,*

1.  $e_{i+1}(T_{i+1}) = \delta$
2.  $\frac{e_{i+2}(T_{i+1})}{\mu^2 \mathbb{E} \delta^2} \rightarrow P_{i+2},$
3.  $e_i(T_{i+1}) = \frac{1-h(T_{i+1})}{h(T_{i+1})} + O(\delta).$
4.  $e_j(T_{i+1}) = o(\delta)$  for  $j < i$ .

Conclusion 1 of Lemma 5.2 follows from the definition of  $T_{i+1}$ . Assuming conclusion 1, we see that variants  $v_{i+1}, v_{i+2}$  remain at  $O(\delta)$  levels throughout  $[T_i^h, T_{i+1}]$ . As a result, the approximate equilibrium of  $e_i, h$  which exists at  $T_i^h$  is maintained. Further, variants  $v_j$  for  $j < i$  continue to drop in number as they are less fit than  $v_i$  variants. These observations justify Conclusions 3 and 4.

We have left to consider Conclusion 2. From (2.12) we have the following ODEs for  $e_{i+1}, e_{i+2}$ ,

$$de_{i+1} = \gamma e_{i+1} (h - \frac{k_{i+1}}{\gamma}), \quad (5.12)$$

$$de_{i+2} = \frac{1}{\mathbb{E}} \left( dP(\gamma h \mathbb{E} e_{i+2} h) - dP(k_{i+2} \mathbb{E} e_{i+2}) + dP(\mu \gamma h \mathbb{E} e_{i+1}) \right).$$

Note that  $e_{i+1}$  is given by a deterministic ODE because  $\mathbb{E}e_{i+1}(T_i) \rightarrow \infty$ . By conclusion 3, since  $e_i, h$  are near equilibrium, we know  $h = k_i/\gamma + O(\delta)$ . Plugging this result into (5.12) gives,

$$\begin{aligned} de_{i+1} &= (\Delta k + O(\delta))e_{i+1}, \\ de_{i+2} &= \frac{1}{\mathbb{E}} \left( dP((k_i + O(\delta))\mathbb{E}e_{i+2}) - dP(k_{i+2}\mathbb{E}e_{i+2}) + dP(\mu(k_i + O(\delta))\mathbb{E}e_{i+1}) \right). \end{aligned} \quad (5.13)$$

If we label the number of  $v_{i+2}$  variants as  $e_{i+2}^\#$ , by our scaling  $e_{i+2}^\# = \mathbb{E}e_{i+2}$ , the  $e_{i+2}$  equation in (5.13) transforms into,

$$de_{i+2}^\# = dP((k_i + O(\delta))e_{i+2}^\#) - dP(k_{i+2}e_{i+2}^\#) + dP(\mu(k_i + O(\delta))\mathbb{E}e_{i+1}), \quad (5.14)$$

and we find that  $v_{i+2}$  variants evolve according to a binary branching process with birth rate  $k_i + O(\delta)$ , death rate  $k_{i+2}$ , and mutation rate that creates new  $v_{i+2}$  variants  $\mu(k_i + O(\delta))\mathbb{E}e_{i+1}$ .

Ignoring the  $O(\delta)$  term in the rates, the growth rate for  $v_{i+2}$  variants, which we label as  $r_{i+2}$ , is  $r_{i+2} = k_i - k_{i+2} = 2\Delta k$ . Considering  $v_{i+1} \rightarrow v_{i+2}$  mutations, we have for the rate

$$\begin{aligned} \text{rate } v_{i+1} \rightarrow v_{i+2} \text{ at time } t &\approx \mu k_i \mathbb{E}e_{i+1}(t) \\ &= \mu k_i \mathbb{E}e_{i+1}(T_i^h) \exp[\Delta k(t - T_i^h)]. \end{aligned} \quad (5.15)$$

By the assumptions of Lemma 5.2, there are no  $v_{i+2}$  variants at time  $T_i^h$ . The  $v_{i+2}$  population arises from mutations in the  $v_{i+1}$  population which expands at rate  $\Delta k$ . Such mutations produce  $v_{i+2}$  cells that then expand at rate  $2\Delta k$ , precisely the generalized LD dynamics mentioned in the Results section.

We define  $\text{LD}_{\text{classic}}(t)$  to be the number of mutants at time  $t$  for the LD model in which mutants and wild types grow at the same rate. In [16, 23] the following asymptotic formula was derived under the further assumptions that wild types grow deterministically and mutants grow stochastically, but with no death events.

$$\text{LD}_{\text{classic}}(t) \approx m \log(m) + m\mathcal{S}(1, 1, \frac{\pi}{2}) \quad (5.16)$$

where  $m$  is the expected number of mutations on the time interval  $[0, t]$  for a wild type population that is of size 1 at time 0. The relative error of (5.16) goes to 0 as  $m \rightarrow \infty$ .

In contrast to  $\text{LD}_{\text{classic}}(t)$ , we let  $\text{LD}_2(t)$  be the number of mutants at time  $t$  for the generalized LD model in which mutants grow at double the rate of wild types. As in the case of  $\text{LD}_{\text{classic}}$ , we will assume that wild types grow deterministically, matching the deterministic growth of  $v_{i+1}$  variants as they spawn. However, for  $\text{LD}_2$  we will assume that mutants have non-zero birth and death rates, corresponding to the situation for  $v_{i+2}$  variants. In section A.2 of the appendix, using generalizations of the techniques found in [23], we show

$$\text{LD}_2(t) \approx m^2 S(\frac{1}{2}, 1, \pi^2 \left( \frac{\Delta k}{k_i} \right)). \quad (5.17)$$

As for (5.16), the relative error of (5.17) goes to 0 as  $m \rightarrow \infty$ .

$e_{i+2}^\#(t)$  is approximately an  $\text{LD}_2(t)$  process on  $[T_i^h, T_{i+1}]$  and becomes exactly so in the SPL. In this setting,  $m$  is the expected number of  $v_{i+1} \rightarrow v_{i+2}$  mutations during  $[T_i^h, T_{i+1}]$ . We show in section A.2 of the appendix,  $m \approx (\frac{k_i \delta}{\Delta k}) \mu \mathbb{E}$ . Plugging this value of  $m$  into (5.17), we find

$$e_{i+2}^\#(T_{i+1}) = \left( \frac{k_i}{\Delta k} \right)^2 \mu^2 \mathbb{E}^2 \delta^2 \mathcal{S}\left(\frac{1}{2}, 1, \pi^2 \left( \frac{\Delta k}{k_i} \right)\right). \quad (5.18)$$

Recalling that  $e_{i+2}(t) = e_{i+2}^\#(t)/\mathbb{E}$  gives conclusion 2 of Lemma 5.2.

## 5.2 Lineage Construction

To demonstrate Theorem 3.1, we need some additional lineage notation. Recall that we consider  $n$  lineages,  $\ell_j$  for  $j = 1, 2, \dots, n$ , corresponding to the  $n$  sampled cells. We let  $\ell_j(t)$  be the ancestral cell at time  $t$  of sample cell  $j$ . (To make this precise we could number the cells in our process as they are born, and then  $\ell_j(t)$  would map to  $\mathbb{N}$ , but we will not make this explicit.) We let  $\mathcal{V}(\ell_j(t))$  be the variant type of  $\ell_j(t)$ . For example,  $\mathcal{V}(\ell(T_{\text{sample}})) = \mathbf{11} \dots \mathbf{1}$ . We write  $\ell_j$ , dropping the time dependence, when we are considering the lineage over a range of times.

To combine the separate lineages into a genealogy, we need to identify mutation and coalescent events. A *mutation event* on  $\ell_j$  occurs at time  $t$  if the variant of  $\ell_j$  changes at time  $t$ , more precisely  $\mathcal{V}(\ell_j(t-)) \neq \mathcal{V}(\ell_j(t))$ . Given two lineages  $\ell_j, \ell_k$ , the lineages have *coalesced by time  $t$*  if  $\ell_j(t) = \ell_k(t)$  and we say that the lineages *coalesced at time  $t$*  if for  $t' > t$ ,  $\ell_j(t') \neq \ell_k(t')$ .

We prove Theorem 3.1 by considering mutation and coalescent events on the interval  $[T_i, T_{i+1}]$ . Lemma 5.3 sets up this analysis by showing that no mutation or coalescent events occur on  $[T_{\mathbf{e}-1}, T_{\text{sample}}]$ . This allows us to consider the interval  $[T_{\mathbf{e}-2}, T_{\mathbf{e}-1}]$  with all lineages of type  $v_{\mathbf{e}}$  at  $T_{\mathbf{e}-1}$ .

Lemma 5.4 provides two results for the general setting of an interval  $[T_i, T_{i+1}]$ , assuming that all lineages are of type  $v_{i+2}$  at  $T_{i+1}$ . First, by time  $T_i$ , all lineages are of type  $v_{i+1}$ . This result implies that each lineage must experience a  $v_{i+1} \rightarrow v_{i+2}$  mutation during  $[T_i, T_{i+1}]$ . Second, two lineages,  $\ell_j, \ell_k$ , coalesce during  $[T_i, T_{i+1}]$  if and only if their associated cells at  $T_{i+1}$ ,  $\ell_j(T_{i+1}), \ell_k(T_{i+1})$ , descend from the same  $v_{i+1} \rightarrow v_{i+2}$  mutation. In other words, the lineages coalesce if there is a cell that is of variant type  $v_{i+1}$  which produces a child cell of type  $v_{i+2}$  from which  $\ell_j(T_{i+1}), \ell_k(T_{i+1})$  are both descended. Lemma 5.4 reduces the analysis of coalescent events on  $[T_i, T_{i+1}]$  to the analysis of mutation events and the number of their descendants at  $T_{i+1}$ .

(5.18) gives an asymptotic description for the number of descendants at  $T_{i+1}$  produced by all  $v_{i+1} \rightarrow v_{i+2}$  mutations during  $[T_i, T_{i+1}]$ . In other words, the pop value of  $v_{i+2}$ . Lemma 5.5 describes  $\Pi(T_i)$  given  $\Pi(T_{i+1})$  by considering each such mutation separately. To do this, we decompose (5.18) into a collection of single mutation results as described in (3.16). Through this decomposition, by exploiting Lemma 5.4, we characterize coalescent events on  $[T_i, T_{i+1}]$ . By repeatedly applying Lemmas 5.4 and 5.5 we can characterize coalescent events on  $[0, T_{\text{sample}}]$ .

**Lemma 5.3.** *For  $t > T_{e-1}$  and  $j, k = 1, 2, \dots, n$ ,  $\mathcal{V}(\ell_j(t)) = v_e$  (no mutation events occur) and  $\ell_j(t) \neq \ell_k(t)$  if  $j \neq k$  (no coalescent events occur).*

*Proof.* Consider the probability that the  $\ell_j$  lineage experiences a mutation at time  $t > T_{e-1}$ . For such an event to occur, a  $v_{e-1} \rightarrow v_e$  mutation must occur and the resultant  $v_e$  variant must be in the  $\ell_j$  lineage. The rate of  $v_{e-1} \rightarrow v_e$  mutations is given by  $\mu\gamma\mathbb{E}h_{e-1}(t)$  which is trivially bounded by  $O(\mu\mathbb{E})$ . By symmetry the  $v_e$  variant resulting from a mutation is in  $\ell_j$  with probability  $O(\frac{1}{\mathbb{E}e_{\mathbf{e}}(t)})$ . By Proposition 1, for  $t > T_{e-1}$  this probability is bounded above by  $O(\frac{1}{\mu^2\mathbb{E}^2\delta^2})$ . From this we have,

$$\begin{aligned} P(\text{no mutation event on } [T_{e-1}, T_{\text{sample}}]) &= \exp\left[-\int_{T_{e-1}}^{T_{\text{sample}}} ds O\left(\frac{1}{\mu\mathbb{E}\delta^2}\right)\right] \\ &= \exp\left[-O\left(\frac{1}{\mu\mathbb{E}\delta}\right)\right] \rightarrow 1. \end{aligned} \tag{5.19}$$

In the last line above we have used the result  $T_{\text{sample}} - T_{e-1} = O(\delta)$ . To see this note that after  $T_{e-1}$ , the  $v_e$  variants expand deterministically. Arguments similar to those used in Proposition 1 show that  $v_e$  will push  $v_{e-1}$  to  $O(\delta)$  levels in  $O(\delta)$  time.

The argument for no coalescent events is similar. For  $\ell_j, \ell_k$  to coalesce at time  $t$ , a  $v_e$  variant must give birth to a new  $v_e$  child cell, which occurs with rate  $O(\mathbb{E}e_{\mathbf{e}}(t))$  and  $\ell_j(t), \ell_k(t)$  must be, in no particular order, precisely these parent and child cells, which occurs with probability  $O(1/(\mathbb{E}e_{\mathbf{e}}(t))^2)$ . This leads to,

$$\begin{aligned} P(\text{no coalescent event on } [T_{e-2}, T_{\text{sample}}]) &= \exp\left[-\int_{T_{e-1}}^{T_{\text{sample}}} ds O\left(\frac{1}{\mathbb{E}e_{\mathbf{e}}(s)}\right)\right] \\ &= \exp\left[-O\left(\frac{\delta}{\mu^2\mathbb{E}^2\delta^2}\right)\right] \rightarrow 1. \end{aligned} \tag{5.20}$$

□

As mentioned, Lemma 5.3 allows us to consider  $[T_i, T_{i+1}]$  under the assumption that all lineages are of type  $v_{i+2}$  at  $T_{i+1}$ . With this in mind, we introduce the following definitions.

$$\begin{aligned} \tau_j &= \inf\{t : \mathcal{V}(\ell_j(t)) = v_{i+2}\}, \\ a_j &= \ell_j(\tau_j). \end{aligned} \tag{5.21}$$

$\tau_j$  is the time of the  $v_{i+1} \rightarrow v_{i+2}$  mutation event on  $\ell_j$  and  $a_j$  is the specific infected cell, a  $v_{i+1}$  variant, that produces the cell  $\ell_j(\tau_j)$ , a  $v_{i+2}$  variant. We use  $a_j$  as a mnemonic for 'ancestor' since  $a_j$  will be the ancestor of  $\ell_j(T_{i+1})$ .

**Lemma 5.4.** *Let  $j, k \in \{1, 2, \dots, n\}$  and assume  $\mathcal{V}(\ell_j(T_{i+1})) = v_{i+2}$  for all  $j$ . Then  $\tau_j \in [T_i, T_{i+1}]$  (a  $v_{i+1} \rightarrow v_{i+2}$  mutation occurs on  $[T_i, T_{i+1}]$ ) and  $\mathcal{V}(\ell_j(T_i)) = v_{i+1}$ . Further for  $j \neq k$ ,  $\ell_j(T_i) = \ell_k(T_i)$  (a coalescent event has occurred) if and only if  $a_j = a_k$ .*

*Proof.* Proposition 1 shows that no  $v_{i+2}$  variants exist at time  $T_i$ , so  $\mathcal{V}(\ell_j(T_i)) \neq v_{i+2}$ . This immediately implies that  $\tau_j \in [T_i, T_{i+1}]$ . For  $t \in [T_i, \tau_j]$ , essentially the same arguments that gave Lemma 5.3 show that no  $v_{i+1}$  variant lineages experience mutation events prior to  $T_i$ . Consequently, we can conclude  $\mathcal{V}(\ell_j(T_i)) = v_{i+1}$ .

Now we consider coalescent events. If  $\tau_j = \tau_k$  then we have  $a_j = a_k$  as required by the lemma. So now assume  $\tau_j > \tau_k$ , we want to show that the two lineages do not coalesce prior to  $T_i$ . Since  $\tau_j \neq \tau_k$ ,  $\ell_j$  and  $\ell_k$  cannot coalesce during  $[\tau_j, T_{i+1}]$ , otherwise we would necessarily have  $\tau_j = \tau_k$ . Further since  $\ell_j$  and  $\ell_k$  are of different variant type during  $(\tau_k, \tau_j]$ , no coalescent event occurs on  $(\tau_k, \tau_j]$ . On the interval  $[T_i, \tau_k)$ ,  $\ell_k, \ell_j$  are of type  $v_{i+1}$  and the same arguments that gave Lemma 5.3 show that  $v_{i+1}$  variants do not coalesce prior to  $T_i$ . We are left with the possibility of a coalescent event at time  $\tau_k$ . This would mean that  $\ell_j(\tau_k-)$ , which is of type  $v_{i+1}$ , produces a mutant child cell that is of type  $v_{i+2}$  which is precisely  $\ell_k(\tau_k)$ . However, the mutation event associated with  $\ell_k(\tau_k)$  is equally likely to be produced by any variant  $v_{i+1}$  at time  $\tau_k$ . The probability that  $\ell_j(\tau_k-)$  is the cell chosen is  $\frac{1}{\mathbb{E}e_{i+1}(\tau_k)}$  which is bounded as follows,

$$\frac{1}{\mathbb{E}e_{i+1}(\tau_k)} < \frac{1}{\mathbb{E}e_{i+1}(T_i)} = \frac{1}{O(\mu^2 \mathbb{E}^2 \delta^2)} \rightarrow 0. \quad (5.22)$$

□

The random partition  $\Xi_{A,i}$  characterizes the coalescent events that occur on  $[T_i, T_{i+1}]$ . From Lemma 5.4, we know that coalescent events are associated with  $v_{i+1} \rightarrow v_{i+2}$  mutations during  $[T_i, T_{i+1}]$ . Mutations that occur relatively early in this time interval will, on average, produce more descendants at  $T_{i+1}$ . Consequently a lineage,  $\ell_j$ , is more likely to descend from a mutation that occurs relatively early. The parameter  $A$  considers mutations that happen on the interval  $[T_i, T_A]$  where  $T_A$  is defined as the time at which the mean number of  $v_{i+1} \rightarrow v_{i+2}$  mutations that are expected to occur is precisely  $A$ . Lemma 5.5 shows that the error in the approximation  $\Xi_{A,i}$  collapses as  $A \rightarrow \infty$ .

**Lemma 5.5.** *Let  $\Delta$  be a fixed partition of  $\Pi(T_{i+1})$  and  $A$  a fixed constant. Then,*

$$\lim P(\Pi(T_i) = \Delta) = P(\Xi_{A,i}(\Pi(T_{i+1})) = \Delta) + O\left(\frac{1}{A}\right). \quad (5.23)$$

*Proof.* Let  $m$  be the mean number of  $v_{i+1} \rightarrow v_{i+2}$  mutations on  $[T_i, T_{i+1}]$  and  $K_{\text{all}}$  a Poisson r.v. with mean  $m$ . Then there are  $K_{\text{all}}$  such mutations. Numbering the mutations in some arbitrary way, we let  $e_{i+2}^{\#, (q)}(T_{i+1})$  be the number, unscaled, of ancestors at  $T_{i+1}$  that descend from mutation  $q$ . The total  $v_{i+2}$  population at  $T_{i+1}$  is then given by,

$$\mathbb{E}e_{i+2}(T_{i+1}) = \sum_{q=1}^{K_{\text{all}}} e_{i+2}^{\#, (q)}(T_{i+1}) \quad (5.24)$$

We split the interval  $[T_i, T_{i+1}]$  into the intervals  $[T_i, T_A]$  and  $[T_A, T_{i+1}]$ . We let  $m_{\text{error}}$  be the mean number of mutations in  $[T_A, T_{i+1}]$ . As mentioned,  $T_A$  is chosen so that the mean number of mutations in  $[T_i, T_A]$



is  $A$ . Then, we have  $m = A + m_{\text{error}}$ . Let  $\mathcal{M}_A$  and  $\mathcal{M}_{\text{error}}$  be the set of mutations that occur on  $[T_i, T_A]$ ,  $[T_A, T_{i+1}]$  respectively. Then (5.24) becomes

$$\mathbb{E}e_{i+2}(T_{i+1}) = \sum_{q \in \mathcal{M}_A} e_{i+2}^{\#, (q)}(T_{i+1}) + \sum_{q' \in \mathcal{M}_{\text{error}}} e_{i+2}^{\#, (q')}(T_{i+1}), \quad (5.25)$$

In section A.3 of the appendix we show,

$$\frac{\sum_{q \in \mathcal{M}_{\text{error}}} e_{i+1}^{\#, (q)}(T_{i+1})}{\sum_{q \in \mathcal{M}_A} e_{i+2}^{\#, (q')}(T_{i+1})} \rightarrow O\left(\frac{1}{A}\right), \quad (5.26)$$

and (5.25) reduces to

$$\mathbb{E}e_{i+2}(T_{i+1}) \approx \sum_{q \in \mathcal{M}_A} e_{i+2}^{\#, (q)}(T_{i+1}). \quad (5.27)$$

A simple computation shows that the number of  $\mathcal{M}_{\text{error}}$  mutations is  $O(\mu E)$  while the number of  $\mathcal{M}_A$  mutations is almost by definition  $O(A)$ . However,  $\mathcal{M}_A$  mutations happen early allowing their descendant population to expand at rate  $2\Delta k$  for a longer time than  $\mathcal{M}_{\text{error}}$  mutations. On the other hand, the lateness of  $\mathcal{M}_{\text{error}}$  mutations means there will be more such mutations because the  $v_{i+1}$  population expands at rate  $\Delta k$ . Since the  $v_{i+1}$  population expands at half the rate of the  $v_{i+2}$  population, the descendants of early mutations dominate.

From (5.27), in the SPL each lineage cell  $\ell_j(T_{i+1})$  must descend from one of the  $\mathcal{M}_A$  mutations. Notice that  $K$  in Definition 1 is precisely the number of  $\mathcal{M}_A$  mutations. By Lemma 5.4  $\ell_j, \ell_k$  coalesce during  $[T_i, T_{i+1}]$  if and only if they descend from the same mutation. Lineage  $j$  descends from mutation  $q$  with probability,

$$\frac{e_{i+2}^{\#, (q)}(T_{i+1})}{\sum_{q'=1}^K e_{i+2}^{\#, (q')}(T_{i+1})}. \quad (5.28)$$

In section A.3 of the appendix through branching process asymptotics we show

$$e_{i+2}^{\#, (q)}(T_{i+1}) \rightarrow C\Gamma^{(i)} \quad (5.29)$$

where  $C$  is a constant that is independent of  $q$ , and  $\Gamma^{(i)}$  is as defined in the Results section just prior to Definition 1. Combining (5.27) and (5.29) gives the pop value decomposition (3.16) stated in the Results section. The constant  $C$  cancels out in the ratio (5.28) and the resultant formula is precisely the 'coloring' probability given in Definition 1. Putting all these observations together proves the lemma.  $\square$

As mentioned in the Results section, we do not sample pop values even though (5.6) would allow it. Crucially, if we sampled pop values then to construct lineages we would need to determine  $e_{i+2}^{\#, (q)}(T_{i+1})$  conditioned on the pop value  $e_{i+2}(T_{i+1})$ . We do not know how to sample from this conditional distribution, so instead we sample  $\Gamma^{(i)}$  which is proportional to  $e_{i+2}^{\#}(T_{i+1})$  (by (5.29)) and thereby implicitly sample  $e_{i+2}(T_{i+1})$  through the decomposition (3.16). Finally we note that the  $C$  in (5.29) is difficult

to compute as it depends on  $h$ . Fortunately, lineage construction can proceed without knowing  $C$ .

Lemmas 5.3-5.5 demonstrate Theorem 3.1. Starting at  $T_{\text{sample}}$ , Lemma 5.3 shows that no coalescent events happen back to  $T_{\mathbf{e}-1}$ . The on each  $[T_i, T_{i+1}]$  for  $i = 0, 1, \dots, \mathbf{e} - 2$  the coalescent events are described by  $\Xi_{A,i}$ . Concatenating these  $\Xi_{A,i}$  takes us back to  $T_0$ . By our assumption on initial conditions, a lemma very similar to 5.3 can be proved showing that no coalescent events occur on  $[0, T_0]$ .

## 6 Full Escape Graph

In this section we generalize the arguments used in Section 5 for the linear escape graph to the full escape graph. As we did for the linear escape graph, we divide the dynamics on the full escape graph into time intervals  $[T_i, T_{i+1}]$ . For the linear escape graph, the  $i$ th variant class,  $\mathcal{E}_i$ , is composed of a single variant  $v_i$  and the  $T_i$  are defined by  $e_i(T_i) = \delta$  in (5.1). To generalize this definition to the full escape graph, we let  $T_i$  be the first time any of the variant populations in class  $i$  reaches a scaled population size  $\delta$ :

$$T_i = \inf\{t : \exists v \in \mathcal{E}_i \text{ such that } e_v(t) \geq \delta\}. \quad (6.1)$$

Sections 6.1 and 6.2 generalize the results for the linear escape graph to the full escape graph. The arguments are similar, so we emphasize the novel ideas that apply to the full escape graph case. As in section 5, we base our analysis on consideration of an interval  $[T_i, T_{i+1}]$ .

### 6.1 Dynamics

During  $[T_i, T_{i+1}]$ , for the linear escape graph, only  $v_{i+1}$  variants spawn  $v_{i+2}$  variants. Recalling that  $\mathcal{P}(v)$  is the set of variant types that can mutate into variant  $v \in \mathcal{E}_{i+2}$ , for the full escape graph all  $v' \in \mathcal{P}(v)$  spawn  $v$  variants. For example **1100** can be spawned by **1000** or **0100**. Consequently, the pop value result, (5.6), must be generalized as follows,

$$\frac{e_v(T_{i+1})}{\mu^2 \mathbb{E} \delta^2} \rightarrow P_v \quad (6.2)$$

where

$$P_v = \sum_{v' \in \mathcal{P}(v)} P_{v' \rightarrow v} \quad (6.3)$$

and

$$P_{v' \rightarrow v} = \left( \frac{P_{v'}}{P_{\max, i+1}} \right)^2 \left( \frac{\Delta k}{k_i} \right)^2 \mathcal{S}\left(\frac{1}{2}, 1, \pi^2 \left( \frac{\Delta k}{k_i} \right)\right). \quad (6.4)$$

where

$$P_{\max, i+1} = \max_{v'' \in \mathcal{E}_{i+1}} P_{v''}. \quad (6.5)$$

With  $P_v$  generalized from (5.7) to (6.4), a version of Proposition 1 generalized in a similar way holds for the full escape graph. Namely, during  $[T_i, T_{i+1}]$  variants in  $\mathcal{E}_i$  sweep to dominance, pushing the  $\mathcal{E}_{i-1}$  to  $O(\delta)$

levels. Concurrently,  $\mathcal{E}_{i+1}$  variants rise to  $O(\delta)$  levels while spawning  $\mathcal{E}_{i+2}$  variants. Spawning events occur for every  $v \in \mathcal{E}_{i+2}$ ,  $v' \in \mathcal{P}(v)$  pair and conclusion 2 of Proposition 1 is generalized to include all such  $P_{v' \rightarrow v}$  pop values as described in (6.2)-(6.4)

Notice that the difference between (6.4) and (5.7) is the factor  $(P_{v'}/P_{\max,i+1})^2$  in (6.4). As this difference is the main technical novelty in moving from a linear to a full escape graph, we focus on its derivation.

At time  $T_i$ , all variants  $v' \in \mathcal{E}_{i+1}$  have  $e_{v'}(T_i) \approx P_{v'}\mu\mathbb{E}\delta^2$ . Consequently, since  $\mathbb{E}e_{v'}(T_i) \rightarrow \infty$  the  $e_{v'}$  dynamics are deterministic in the SPL and we have,

$$\frac{e_{v'}(t)}{\mu^2\mathbb{E}\delta^2} \approx P_{v'}I_{v'}(t) \quad (6.6)$$

where

$$I_{v'}(t) = \exp\left[\int_{T_i}^t ds(\gamma h(s) - k_{i+1}]\right]. \quad (6.7)$$

Notice that  $I_{v'}(t)$  is dependent only on the variant class  $\mathcal{E}_{i+1}$  through  $k_{i+1}$  but not on the specific variant  $v'$  in  $\mathcal{E}_{i+1}$ . This leads to the ratio for  $v', v'' \in \mathcal{E}_{i+1}$ ,

$$\frac{e_{v'}(T_{i+1})}{e_{v''}(T_{i+1})} = \frac{P_{v'}}{P_{v''}}. \quad (6.8)$$

Recall that  $T_{i+1}$  is defined as the first time for which some variant  $v' \in \mathcal{E}_{i+1}$  is of scaled population size  $\delta$ . Let  $v_{\max,i+1}$  be that variant. Then, by definition

$$e_{v_{\max,i+1}}(T_{i+1}) = \delta, \quad (6.9)$$

Further, from (6.6) we know that  $P_{v_{\max,i+1}} = P_{\max,i+1}$ . Plugging the equation directly above into (6.8) with  $v'' = v_{\max,i+1}$  gives

$$e_{v'}(T_{i+1}) = \left(\frac{P_{v'}}{P_{\max,i+1}}\right)\delta. \quad (6.10)$$

The  $v'$  population size at  $T_i$  is too small to create  $v' \rightarrow v$  mutations (this is the content of conclusions 1 and 2 in Lemma 5.1). Consequently, if we want to know how many  $v$  variants are produced at  $T_{i+1}$  by  $v' \rightarrow v$  mutations and their descendants, all we have to know is  $e_{v'}(T_{i+1})$ . Indeed, the arguments of section 5 show that when  $e_{v'}(T_{i+1}) = \delta$ , then  $e_v(T_{i+1}) = \mu^2\mathbb{E}\delta^2\mathcal{S}$ . But for the full escape graph,  $e_{v'}(T_{i+1})$  is given by (6.10) and consequently we must replace  $\delta$  by  $(P_{v'}/P_{\max,i+1})\delta$  in (5.7). This substitution gives (6.4).

## 6.2 Lineage Construction

Lemmas 5.3 and 5.4 proved for the linear escape graph apply to the full escape graph with almost identical proofs. Lemma 5.5, on the other hand, requires significant generalization.

In the case of the linear escape graph, given an  $A$  we defined  $T_A$  on the  $[T_i, T_{i+1}]$  interval as the time at which the number of  $v_{i+1} \rightarrow v_{i+2}$  mutations has mean  $A$ . More precisely,  $T_A$  was defined by,

$$\int_{T_i}^{T_A} ds(\mu\gamma h\mathbb{E})e_{v_{i+1}}(s) = A. \quad (6.11)$$

For the full escape graph, we generalize the definition of  $T_A$  by considering the variant  $v_{\max, i+1}$  (defined in the previous subsection):

$$\int_{T_i}^{T_A} ds (\mu \gamma h \mathbb{E}) e_{v_{\max, i+1}}(s) = A. \quad (6.12)$$

Using (6.8) with  $T_{i+1}$  replaced by  $T_A$  we find that the mean number of  $v' \rightarrow v$  mutations produced by  $T_A$  is  $A(P_{v'}/P(v_{\max, i+1}))$ . In other words, each  $v'$  has an associated scaled version of  $A$ .

For the linear escape graph, we sampled  $K \sim \text{Poisson}(A)$  versions of  $\Gamma^{(i)}$  and then applied the paintbox construction given by Definition 1. For the full escape graph, the idea is similar except that for each  $v'$  such that  $v' \rightarrow v$  mutations are possible we must take  $\text{Poisson}(A(P_{v'}/P(v_{\max, i+1})))$  samples of  $\Gamma^{(i)}$ . Then, we must assign different 'colors' for each such sample for each possible  $v'$ .

Everything then proceeds according to a paintbox partition, except that the colors also tell us which variant in the  $\mathcal{E}_{i+1}$  class produced the lineage being colored. So, as described by Definition 3, we must not only coalesce lineages according to the paintbox construction, we must also allocate the lineages to the appropriate  $\mathcal{E}_{i+1}$  variants at time  $T_i$ .

To implement all this, we estimate pop values through the decomposition  $D_v$  given in (3.21). As we mentioned directly below the proof of Lemma 5.5, we do not sample pop values directly using (6.2) because then we would need to consider conditional distributions from which we do not know how to sample. Notice that  $K_{v' \rightarrow v}$  depends only on the ratio of pop values, and so we may use the  $D_v$  to form  $K_{v' \rightarrow v}$ . Since we take all  $\mathcal{E}_1$  variants to be of equal population size at  $t = 0$ , we may take  $D_v = 1$  for  $v \in \mathcal{E}_1$  to start the iteration. Once  $D_v$  and the  $\Gamma^{(i)}$  have been sampled according to Definition 2, we move backwards from  $T_{\text{sample}}$  to  $T_0$  and implement the paintbox construction of the  $\Xi_{A, i}$ , Definition 3, in order to coalesce lineages.

## A Appendix

### A.1 Proof of Lemma 5.1

In this section, we provide the technical details that support conclusions 3 and 4 of Lemma 5.1. From conclusions 1 and 2, we know  $e_i, e_{i+1} \ll \delta$  and we can reduce (2.12) to the following,

$$\begin{aligned} \frac{dh}{dt} &= g(1 - h - h(e_i + e_{i-1} + o(\delta))) \\ \frac{de_i}{dt} &= \gamma e_i \left(h - \frac{k_i}{\gamma}\right) + O(\mu) \\ \frac{de_{i-1}}{dt} &= \gamma e_{i-1} \left(h - \frac{k_{i-1}}{\gamma}\right) + O(\mu). \end{aligned} \quad (\text{A.1.1})$$

The  $O(\mu)$  terms in the last two equations directly above can be ignored because  $T_i^h - T_i = O(|\log(\delta)|)$  and  $\mu |\log(\delta)| \rightarrow 0$ . Dropping these terms,

we note the following relation,

$$\frac{d(\log(e_i) - \log(e_{i-1}))}{dt} = \Delta k. \quad (\text{A.1.2})$$

Integrating the above equation and using our assumptions on  $e_{i-1}(T_i)$  and  $e_i(T_i)$  we find,

$$\frac{e_i(t)}{e_{i-1}(t)} = O(\delta \exp[\Delta k(t - T_i)]). \quad (\text{A.1.3})$$

If we can show that  $e_i$  is bounded then as  $t$  grows, (A.1.3) implies that  $e_{i-1}$  collapses. To see that  $e_i$  is bounded, set

$$z(t) = \frac{h(t)}{g} + \frac{e_i(t)}{\gamma} + \frac{e_{i-1}(t)}{\gamma} \quad (\text{A.1.4})$$

Then by straightforward differentiation,

$$\begin{aligned} \frac{dz}{dt} &= 1 - h - h \cdot o(\delta) - e_i \frac{k_i}{\gamma} - e_{i-1} \frac{k_{i-1}}{\gamma} \\ &\leq 1 - \min(g(1 - o(\delta)), k_i, k_{i-1})z \end{aligned} \quad (\text{A.1.5})$$

Since  $z(t)$  is non-negative, we find that  $z(t)$  must be bounded. In turn  $h$ ,  $e_i$  and  $e_{i-1}$  must be bounded. Returning to (A.1.3) and setting  $t \geq 2/|\Delta k| \log(\delta)$  we find, since  $e_i$  is bounded,

$$e_{i-1}(t) = O(\delta). \quad (\text{A.1.6})$$

Once  $t > 2/|\Delta k| \log(\delta)$ , we can further reduce (A.1.1) to,

$$\begin{aligned} \frac{dh}{dt} &= g(1 - h - h(e_i + O(\delta))) \\ \frac{de_i}{dt} &= \gamma e_i(h - \frac{k_i}{\gamma}) \end{aligned} \quad (\text{A.1.7})$$

Consider then (A.1.7). Ignoring the  $O(\delta)$  term for a moment, the system is not dependent on  $\delta$ . Since we have shown  $h, e_i$  to be bounded, application of Poincare-Bendixon shows that the system converges to its non-trivial equilibrium,  $h = \frac{k_i}{\gamma}$  and  $e_i = \frac{1-h}{h}$ . Now consider the  $O(\delta)$  term. Given some fixed distance  $\epsilon > 0$ , if we run the system from  $t = 2/|\Delta k| \log(\delta)$  to  $t = 3/|\Delta k| \log(\delta)$  we are guaranteed by choosing  $\delta$  sufficiently small to be within  $\epsilon$  of the equilibrium. In turn, taking  $\epsilon$  small, we can linearize (A.1.7) about its equilibrium.

Straightforward computation shows that both eigenvalues of the linearized system have negative real part bounded above by,

$$\rho = -(g\gamma + O(\delta)) \min(1, \frac{4k^2}{g\gamma}(1 - \frac{k}{\gamma})) \quad (\text{A.1.8})$$

Running the system from  $t = 3/|\Delta k| \log(\delta)$  to  $t = (3 + \frac{2}{|\rho|})|\log(\delta)|$  forces (A.1.7) to within  $O(\delta)$  of the equilibrium.

## A.2 Proof of (5.18)

In this section we provide technical details that justify (5.18). (5.18) is what underlies our pop value formulas. The arguments we employ are extensions of those found in [23] which considered the  $\text{LD}_{\text{classic}}(t)$  process. To make this connection more explicit, where possible we adopt the notation of [23].

Following from the arguments made directly above (5.15), we assume the following:

1. the  $v_{i+1}$  population expands deterministically from time  $T_i^h$  to  $T_{i+1}$  with rate  $\Delta k + O(\delta)$
2. at time  $T_i^h$  no  $v_{i+2}$  variants exist
3.  $v_{i+1} \rightarrow v_{i+2}$  mutations occur at rate  $\mu k_i E e_{i+1}$ .
4.  $v_{i+2}$  variants have birth and death rates  $b = k_i + O(\delta)$  and  $d = k_{i+2} + O(\delta)$ .

We set  $r = b - d$  and by our assumptions on CTL attack,  $r = 2\Delta k + O(\delta)$ . We will develop our formulas for arbitrary  $b, d$  assuming only  $r > \Delta k$ .

As observed in [23], the number of mutations is Poisson distributed with mean  $m$  given by,

$$m = \int_{T_i^h}^{T_{i+1}} ds \mu k_i \mathbb{E} e_{i+1}(T_i^h) \exp[(\Delta k + O(\delta))(s - T_{i+1})] \quad (\text{A.2.9})$$

By definition  $e_{i+1}(T_{i+1}) = \delta$ . We can then estimate the integral expression for  $m$  and find,

$$m = \left(\frac{k_i}{\Delta k}\right) \mu \mathbb{E} \delta \exp[O(\delta)(T_{i+1} - T_i^h)]. \quad (\text{A.2.10})$$

We want to show that  $\exp[O(\delta)(T_{i+1} - T_i^h)] \rightarrow 1$ . Note the following three facts,

- $e_{i+1}(T_{i+1}) = \delta$
- $e_{i+1}(T_i^h) > e_{i+1}(T_i) = O(\mu^2 \mathbb{E} \delta^2)$
- On  $[T_i^h, T_i]$ ,  $e_{i+1}$  grows deterministically with rate  $\Delta k + O(\delta)$ ,

In other words, we know where  $e_{i+1}$  starts and ends, and we know its growth rate. Then, we can find the bound

$$T_{i+1} - T_i \leq O\left(\frac{1}{|\log(\mu^2 E \delta^2)|}\right). \quad (\text{A.2.11})$$

And so by our definition of  $\delta$ , (5.2), we can conclude  $\exp[O(\delta)(T_{i+1} - T_i^h)] \rightarrow 1$ . Plugging this observation into (A.2.10) gives,

$$\frac{m}{\left(\frac{k_i}{\Delta k}\right) \mu \mathbb{E} \delta} \rightarrow 1. \quad (\text{A.2.12})$$

A similar argument will show that the  $O(\delta)$  expressions in the formulas for  $b, d$  and mutation rate will have no effect in the SPL. For simplicity then, we drop  $O(\delta)$  terms from this point on without comment.

Connecting to the notation of [23], we let  $Y_m = e_{i+2}^\#(T_{i+1})$ , the number of  $v_{i+2}$  variants at time  $T_{i+1}$ . We can decompose  $Y_m$  by

$$Y_m = \sum_{k=1}^K X_k, \quad (\text{A.2.13})$$

where  $K$  is Poisson distributed with mean  $m$ , given in (A.2.10), and each  $X_k$  represents the number of  $v_{i+2}$  variants at time  $T_{i+1}$  that descend from a single  $v_{i+2}$  variant produced by a  $v_{i+1} \rightarrow v_{i+2}$  mutation (compare (2.1) in [23]). Conditioned on  $K$ , the times of the  $K$  mutations are iid. and in turn, the  $X_k$  are iid.

The following lemma characterizes the Laplace transform of  $X_k$ .

**Lemma A.1.** *Let the  $X_k$  be iid versions of the r.v.  $X$ . Recall  $r = b - d$ . Then*

$$\lim_{\lambda \rightarrow 0} \frac{E[\exp[-\lambda X]] - 1}{\lambda^{\frac{\Delta k}{r}}} = -\Upsilon(b, d, \Delta k) \quad (\text{A.2.14})$$

where

$$\Upsilon(b, d, \Delta k) = -\frac{r}{r - \Delta k} \left( \frac{\Delta k}{r} - 1 \right) \left( \frac{\Delta k}{r} \right) \pi \left( \frac{r}{b} \right)^{1 - \frac{\Delta k}{r}} \csc\left(\pi \frac{\Delta k}{r}\right) \quad (\text{A.2.15})$$

Before proving Lemma A.1, we state and demonstrate Proposition A.1 which characterizes the distribution of  $Y_m$  for large  $m$ . (5.17) follows from Proposition A.1 by setting  $r = 2\Delta k$ . (5.18) follows from the proposition by further setting  $m = (k_i/\Delta k)\mu\mathbb{E}\delta$  as justified by (A.2.12).

**Proposition A.1.**

$$\lim_{m \rightarrow \infty} \frac{Y_m}{m^{\frac{r}{\Delta k}}} \rightarrow \mathcal{S}\left(\frac{\Delta k}{r}, 1, \Upsilon(r, \Delta k)\right) \quad (\text{A.2.16})$$

To see that Proposition A.1 follows from Lemma A.1, first notice that by (A.2.13) and the independence of the  $X_k$  we have

$$E[-\lambda Y_m] = \exp[m(E[\exp[-\lambda X]] - 1)]. \quad (\text{A.2.17})$$

Replacing  $\lambda$  by  $\lambda/m^{r/\Delta k}$  in the above equality and applying Lemma A.1 gives,

$$\lim_{m \rightarrow \infty} E[-\lambda \frac{Y_m}{m^{\frac{r}{\Delta k}}}] = \exp[-\lambda^{\frac{\Delta k}{r}} \Upsilon(b, d, \Delta k)]. \quad (\text{A.2.18})$$

Stable distributions are characterized by index  $\alpha$ , the skewness parameter  $\beta$ , and the scale factor  $c$  [24]. The limit above is seen as the Laplace transform of a  $\alpha = \frac{\Delta k}{r}$  stable distribution. Since the support of  $Y_m$  is on  $[0, \infty]$ ,  $\beta = 1$  [24].  $c$  is defined through the characteristic function of the stable process. To determine  $c$  we invert the characteristic function of  $S(\Delta k/r, 1, c)$  and compute its Laplace transform. Setting this result equal to the right side of (A.2.18) we find,

$$c = \left( \Upsilon(b, d, \Delta k) \frac{1 + \cos(\pi\alpha)}{\cos(\frac{\pi\alpha}{2})} \right)^{\frac{1}{\alpha}} \quad (\text{A.2.19})$$

In the case  $\alpha = 1/2$  we find

$$c = 2\Upsilon^2(b, d, \Delta k) \quad (\text{A.2.20})$$

If we plug in our values for  $b, d$  in the formula for  $\Upsilon$  we find

$$\Upsilon = -\frac{\pi}{2} \sqrt{\frac{2\Delta k}{k_i}}, \quad (\text{A.2.21})$$

and so we arrive at

$$c = \pi^2 \left( \frac{\Delta k}{k_i} \right). \quad (\text{A.2.22})$$

Finally, we give the proof of Lemma A.1.

*Proof of Lemma A.1.* Let  $t^*$  be the random time of a single mutation. A standard Poisson process argument applied to (A.2.9) gives for the density of  $t^*$ ,

$$P(t^* = s) = \Delta k \exp[-\Delta k(T_{i+1} - s)], \quad (\text{A.2.23})$$

Let  $Z(t)$  be a branching process with birth and death rates  $b, d$  respectively run to time  $t$  assuming  $Z(0) = 1$ . Then  $X = Z(t^*)$  and we can represent  $E[\exp[-\lambda X]] - 1$  by,

$$E[\exp[-\lambda X]] - 1 = \int_{T_i^h}^{T_{i+1}} ds \Delta k \exp[-\Delta k(T_{i+1} - s)] G(T_{i+1} - s), \quad (\text{A.2.24})$$

where

$$G(t) = \exp[-\lambda Z(t)] - 1. \quad (\text{A.2.25})$$

Extending the range of integration from  $T_i^h$  down to  $-\infty$  also adds error that collapses in the SPL. With this observation and the change of variable  $s \rightarrow T_{i+1} - s$  we consider,

$$E[\exp[-\lambda X]] - 1 = \int_0^\infty ds \Delta k \exp[-\Delta k s] G(s) \quad (\text{A.2.26})$$

To understand (A.2.26), we have found it useful to make the substitution  $w = \lambda \exp[rs]$ . To explain why, we observe the well known fact,  $E[Z(t)] = \exp[rt]$ . We expect then,

$$G(t) \approx \exp[-\lambda \exp[rt]] - 1 = \exp[-w] - 1. \quad (\text{A.2.27})$$

As a result, at least for us, analyzing (A.2.26) in terms of  $w$  simplifies the contribution of the  $G(t)$  term to (A.2.26). Making the substitution gives,

$$E[\exp[-\lambda X]] - 1 = \frac{\Delta k}{r} \lambda^{\frac{\Delta k}{r}} \int_\lambda^\infty dw \frac{1}{w^{1+\frac{\Delta k}{r}}} G(f(w)) \quad (\text{A.2.28})$$

where  $f(w) = \frac{1}{r} \log(\frac{w}{\lambda})$ . The integral to the right of the equality directly above has a limit as  $\lambda \rightarrow 0$ . This is not obvious due to the singularity of  $\frac{1}{w^{1+\frac{\Delta k}{r}}}$  at  $w = 0$ . To remove the singularity and show that the integral



is indeed  $O(1)$  we apply partial integration twice, integrating the  $\frac{1}{w^{1+\frac{\Delta k}{r}}}$  term and differentiating the  $G(f)$  term. We find,

$$E[\exp[-\lambda X]] - 1 = \lambda^{\frac{\Delta k}{r}} \left[ -\frac{r}{r - \Delta k} \int_{\lambda}^{\infty} dw (w^{1-\frac{\Delta k}{r}}) [G(f(w))]'' + I_1 + I_2 \right] \quad (\text{A.2.29})$$

where

$$I_1 = -w^{-\frac{\Delta k}{r}} G(f(w)) \Big|_{\lambda}^{\infty}, \quad (\text{A.2.30})$$

$$I_2 = \left( \frac{r}{r - \Delta k} \right) w^{1-\frac{\Delta k}{r}} [G(f(w))]' \Big|_{\lambda}^{\infty}.$$

$G$  can be characterized through a Kolmogorov equation. In our specific case

$$G' = bG(G + (1 - \frac{d}{b})). \quad (\text{A.2.31})$$

(A.2.31) can be integrated to find a specific formula for  $G$  and using (A.2.29) we find

$$\lim_{\lambda \rightarrow 0} \frac{E[\exp[-\lambda X]] - 1}{\lambda^{\frac{\Delta k}{r}}} = \Upsilon(b, d, \Delta k), \quad (\text{A.2.32})$$

□

### A.3 Proof of Lineage Construction Approximation

In this subsection, we demonstrate the two assertions used to prove Lemma 5.5 which justifies our paintbox construction approximation of  $\Pi(0)$ .

**Lemma A.2.**

$$\frac{\sum_{q' \in \mathcal{M}_{\text{error}}} \mathbb{E} e_{i+1}^{(q')}(T_{i+1})}{\sum_{q \in \mathcal{M}_A} \mathbb{E} e_{i+1}^{(q)}(T_{i+1})} = O\left(\frac{1}{A}\right), \quad (\text{A.3.33})$$

*Proof.* If we sum the numerator and denominator of (A.3.33), we have  $Y_m$  which was introduced in the previous section, see (A.2.13). We know through Proposition A.1 that  $Y_m/m^2$  converges to a stable distribution. We now apply the arguments of Proposition A.1 separately to the numerator and denominator. The difference in the arguments will be that the bounds of integration in (A.2.28) will no longer be  $\lambda$  and  $\infty$ . However the same essential ideas are used and we find,

$$\sum_{q \in \mathcal{M}_A} \mathbb{E} e_{i+2}^{(q)}(T_{i+1}) \approx \left( \frac{\Delta k}{k_i} \right)^2 (\delta \mu \mathbb{E})^2 \mathcal{S}\left(\frac{1}{2}, 1, \pi^2 \left( \frac{\Delta k}{k_i} \right)\right) \quad (\text{A.3.34})$$

while

$$\sum_{q' \in \mathcal{M}_{\text{error}}} \mathbb{E} e_{i+2}^{(q')}(T_{i+1}) \approx O((\delta \mu \mathbb{E})^2) \mathcal{N}\left(\frac{1}{A}, \frac{1}{A^3}\right), \quad (\text{A.3.35})$$

where  $\mathcal{N}(\mu, \sigma^2)$  is a normal distribution with mean  $\mu$  and variance  $\sigma^2$ . Notice that the early mutations produce a heavy tailed distribution, while the later mutations are normally distributed. By time  $T_A$ , the rate of mutation is  $O(A)$ , as a result many mutations happen at approximately the same time and through an appropriate scaling these nearly simultaneous mutations lead to a central limit theorem. Taking the ratio of (A.3.34) and (A.3.35) gives (A.3.33)  $\square$

**Lemma A.3.**

$$\frac{\mathbb{E}e_{i+2}^{(q)}}{\sum_{\mathcal{M}_A} \mathbb{E}e_{i+2}^{(q')}} \rightarrow \frac{\Gamma_q}{\sum_{q' \in \mathcal{M}_A} \Gamma_{q'}}, \quad (\text{A.3.36})$$

where the  $\Gamma_q$  are sampled from  $\Gamma^{(i)}$ .

*Proof.* Let  $t^*$  be the random time of a mutation on  $[T_i^h, T_A]$ . Up to an error that disappears in the limit, we have

$$P(T_A - t^* = s) = \Delta k \exp[-\Delta k s]. \quad (\text{A.3.37})$$

In other words  $T_A - t^*$  is exponentially distributed with rate  $\Delta k$  and setting

$$\xi_{q,2} = \Delta k(T_A - t^*) \quad (\text{A.3.38})$$

defines  $\xi_{q,2}$  as a exponential r.v. with rate 1. When a  $v_{i+1} \rightarrow v_{i+2}$  mutation occurs at time  $t^*$ , the number of descendants at  $T_{i+1}$ ,  $\mathbb{E}e_{i+2}^{(q)}(T_{i+1})$  is given by  $Z(T_{i+1} - t^*)$  (recall the definition of  $Z(t)$  from section A.2). Since  $T_{i+1} - T_A \rightarrow \infty$  and  $t^* < T_A$ , we have  $T_{i+1} - t^* \rightarrow \infty$ . Standard asymptotic results from branching process theory (see [1]) give,

$$\exp[-2\Delta k(T_i - t^*)]Z(T_i - t^*) \rightarrow \frac{k_i}{2\Delta k} \xi_{q,1} B\left(\frac{2\Delta k}{k_i}\right), \quad (\text{A.3.39})$$

where  $\xi_{q,1}$  is exponential with rate 1 and  $B(p)$  is a Bernoulli r.v. with success probability  $p$ . We can apply this analysis to each  $\mathbb{E}e_{i+2}^{(q)}$  in (A.3.36) by multiplying the numerator and denominator by  $\exp[-2\Delta k(T_i - T_A)]$  to find,

$$\begin{aligned} \frac{\mathbb{E}e_{i+2}^{(q)}(T_{i+1})}{\sum_{q \in \mathcal{M}_A} \mathbb{E}e_{i+2}^{(q)}(T_{i+1})} &\rightarrow \frac{\exp[2\Delta k(T_A - t_q^*)] \frac{k_i}{2\Delta k} \xi_{q,1} B_q\left(\frac{2\Delta k}{k_i}\right)}{\sum_{q' \in \mathcal{M}_A} \exp[2\Delta k(T_A - t_{q'}^*)] \frac{k_i}{2\Delta k} \xi_{q',1} B_{q'}\left(\frac{2\Delta k}{k_i}\right)} \\ &= \frac{\exp[2\zeta_{q,2}] \xi_{q,1} B_q\left(\frac{2\Delta k}{k_i}\right)}{\sum_{q' \in \mathcal{M}_A} \exp[2\xi_{q',2}] \xi_{q',1} B_{q'}\left(\frac{2\Delta k}{k_i}\right)} \\ &= \frac{\Gamma_q}{\sum_{q' \in \mathcal{M}_A} \Gamma_{q'}}. \end{aligned} \quad (\text{A.3.40})$$

$\square$

## References

- [1] K.B. Athreya and P.E. Ney. *Branching Processes*. Springer-Verlag, 1972.
- [2] N.H. Barton et al. Coalescence in a random environment. *Ann. App. Prob.*, 14:754–785, 2004.
- [3] P.H. Borrow et al. Virus-specific cd8+ cytotoxic t-lymphocyte activity associated with control of viremia in primary human immunodeficiency virus type 1 infection. *J. Virology*, 68:6103–6110, 1994.
- [4] M. Carrington and S.J. O’Brien. The influence of hla genotype on aids. *AIDS. Annu. Rev. Med.*, 54:535–551, 2003.
- [5] K.A. Crandall. *The Evolution of HIV*. Johns Hopkins University Press, 1999.
- [6] A.L. DeFranco, R.M. Locksley, and M. Robertson. *Immunity: The Immune Response in Infectious and Inflammatory Disease*. New Science Press, 2007.
- [7] A.J. Drummond and A. Rambaut. Beast: Bayesian evolutionary analysis by sampling trees. *BMC Evolutionary Biology*, 7:214, 2007.
- [8] A.J. Drummond and A.G. Rodrigo. Reconstructing genealogies of serial samples under the assumption of a molecular clock using serial-sample upgma. *Mol. Bio. Evol.*, 17:1807–1815, 2000.
- [9] R. Durrett et al. A waiting time problem arising from the study of multi-stage carcinogenesis. *Ann. App. Prob.*, 19(2):676–718, 2009.
- [10] R. Durrett and J. Schweinsberg. Approximating selective sweeps. *Theo. Pop. Bio.*, 66:1291–138, 2004.
- [11] N. Goonetilleke et al. The first t cell response to transmitted/founder virus contributes to the control of acute viremia in hiv-1 infection. *J. Exp. Med.*, 206(6):1253–1272, 2009.
- [12] J. Hermisson and P.S. Pennings. Soft sweeps: Molecular population genetics of adaptation from standing genetic variation. *Genetics*, 169:2335–2352, 2005.
- [13] Y. Iwasa et al. Population genetics of tumor suppressor genes. *J. Theor. Bio.*, 233:15–23, 2005.
- [14] N.L. Kaplan et al. The coalescent process in models with selection. *Genetics*, 120:819–829, 1988.
- [15] A.D. Kelleher et al. Clustered mutations in hiv-1 gag are consistently required for escape from hla-b27-restricted cytotoxic t lymphocyte responses. *J. Exp. Med.*, 193:375–386, 2001.
- [16] T.B. Kepler and M. Oprea. Improved inference of mutation rates : I. an integral representation for the luria-delbruck distribution. *Theo. Pop. Bio.*, 59:41–48, 2001.
- [17] J.F.C. Kingman. Random partitions in population genetics. *Proc. R. Soc. Lond. A.*, 361(1):20, 1978.

- [18] R.A. Koup et al. Temporal association of cellular immune responses with the initial control of viremia in primary human immunodeficiency virus type 1 syndrome. *J. Virology*, 68:4650–4655, 1994.
- [19] M.K. Kuhner. Lamarc 2.0: Maximum likelihood and bayesian estimation of population parameters. *Bioinformatics*, 22(6):768–770, 2006.
- [20] T. Kurtz. *Approximation of Population Processes*, volume 36. CBMS-NSF Regional Conference Series in Applied Mathematics, 1981.
- [21] S. Levisang. Sampling hiv intrahost genealogies based on a model of acute stage ctl response. *Bull. Math. Bio.*, 2011.
- [22] J.A. Levy. *HIV and the Pathogenesis of AIDS. Second Edition*. ASM Press. Washington, DC., 1998.
- [23] M. Mohle. Convergence results for compound poisson distributions and applications to the standard luria-delbruck distribution. *J. Appl. Prob.*, 42(3):620–631, 2005.
- [24] J.P. Nolan. *Stable Distributions - Models for Heavy Tailed Data*. Birkhauser, Boston, 2011. In progress, Chapter 1 online at [academic2.american.edu/~jpnolan](http://academic2.american.edu/~jpnolan).
- [25] M.A. Nowak and R.M. May. *Virus Dynamics: Mathematical Principles of Immunology and Virology*. Oxford University Press, 2000.
- [26] P.S. Pennings and J. Hermisson. Soft sweeps iimolecular population genetics of adaptation from recurrent mutation or migration. *Mol. Bio. Evol.*, 23(5):1076–1084, 2006.
- [27] A.S. Perelson. Modeling viral and immune system dynamics. *Nature Reviews*, 2:28–36, 2002.
- [28] A.S. Perelson et al. Hiv-1 dynamics in vivo: Virion clearance rate, infected cell life-span, and viral generation time. *Science*, 271:1582–1586, 1996.
- [29] J. Pitman. Combinatorial stochastic processes. St Flour Probability Summer School Lecture Notes. Springer, 2002.
- [30] A.G. Rodrigo et al. Coalescent estimates of hiv-1 generation time in vivo. *PNAS*, 96:2187–2191, 1999.
- [31] A.G. Rodrigo and J. Felsenstein. *The Evolution of HIV*. Johns Hopkins University Press, 1999. Chapter: Coalescent Approaches to HIV Population Genetics.
- [32] I.M. Rouzine and J.M. Coffin. Multi-site adaptation in the presence of infrequent recombination. *Theo. Pop. Bio.*, 77:189–204, 2010.
- [33] J.E. Schmitz et al. Control of viremia in simian immunodeficiency virus infection by cd8 + lymphocytes. *Science*, 283:857, 1999.
- [34] Chun T.-W. et al. Quantification of latenet tissue reservoirs and total body viral load in hiv-1 infection. *Nature*, 387:183–188, 1997.
- [35] J. Wakeley. *Coalescent Theory: An Introduction*. Roberts and Company Publishers, 2008.
- [36] Q. Zheng. Progress of a half century in the study of the luria-delbruck distribution. *Math. BioSci.*, 162:1–32, 1999.